# ANALYTICAL STUDY OF ZONE OF PLASTIC AND CRACKED REGION IN SLENDER BRIDGE PIERS USING FINITE ELEMENT METHOD

*A dissertation submitted in fulfillment of the requirement for the award of the degree of*

MASTER OF ENGINEERING

In

Structural Engineering

Submitted By

**HIMANSHU SHARMA**

**801624013**

Under Supervision of

**Dr Prem Pal Bansal**

Head of Civil Engineering Department

(TIET)

and

**Er Aswin Kumar Padhy**

Senior General Manager

(SMEC India Pvt Ltd)


CIVIL ENGINEERING DEPARTMENT

THAPAR INSTITUTE OF ENGINEERING & TECHNOLOGY
(A DEEMED TO BE UNIVERSITY), PATIALA, PUNJAB
JULY, 2018

## DECLARATION

I, Himanshu Sharma hereby declare that the work presented in this dissertation entitled "ANALYTICAL STUDY OF ZONE OF PLASTIC AND CRACKED REGION IN SLENDER BRIDGE PIERS USING FINITE ELEMENT METHOD" in fulfillment of the requirement for the award of degree of Master of Engineering in Structural Engineering, submitted at Civil Engineering Department, Thapar Institute of Engineering & Technology (A Deemed to be University), Patiala is an authentic record of work carried out under joint supervision of Dr Prem Pal Bansal , Associate Professor & the Head, Civil Engineering Department, Thapar Institute of Engineering & Technology, A Deemed to be University, Patiala and Er Aswin Kumar Padhy, Senior General Manager, Highways and Bridges, SMEC India Pvt Ltd, Gurugram, from August 2017 to June 2018. The matter presented in this dissertation has not been submitted either in part or full to any other university or institute for the award of any other degree.

Himanshu Sharma

Date : 4-8-2018

Himanshu Sharma
801624013

**Dr Prem Pal Bansal**
Associate Professor & Head
Civil Engineering Department
Thapar Institute of Engineering & Technology
(A Deemed to be University), Patiala ,Punjab

**Er Aswin Kumar Padhy**
Senior General Manager
Highways and Bridges
SMEC India Pvt Ltd
Gurugram,Haryana

Date : 4-8-2018

# ACKNOWLEDGEMENT

This dissertation would not have been possible without the support of the entire Civil Engineering Department of Thapar Institute of Engineering & Technology, Patiala which provided me an opportunity to pursue industry-oriented research program. The efforts of the department for making this program possible are highly acknowledged.

I would also like to pay my sincere gratitude to my guide Dr. Prem Pal Bansal (Associate Professor & Head ) for his valuable suggestion regarding the selection of a better organization where the purpose of this prestigious program could be effectively accomplished.

I also take this opportunity to acknowledge the entire Highway and Bridge Department of SMEC INDIA PVT LTD, especially Er.Aswin Kumar Padhy (Senior General Manager) for discussing various areas of practical design which still need improvement and helping me decide an industry-oriented dissertation topic. The efforts of entire team of engineers and draftsmen who helped me in clearing various doubts I came across in routine work in the company are also acknowledged.

Last but not the least I thank my parents and friends for being a great moral support, helping me maintain a low stress level that ensured proper concentration on the work.

Himanshu Sharma

801624013

# ABSTRACT

The performance of slender bridge piers when subjected to lateral loads acting simultaneously with axial loads is a significant issue faced by the bridge design industry. For such piers the interaction of flexural ductility with the variation in lateral and longitudinal reinforcement is not well established. The precise height up to which lateral confinement should be provided to ensure adequate ductility in seismic scenarios is still a topic of research for slender piers. While most of the international codes have given general guidelines for the height of lateral confinement in bridge piers , the adequacy of these guidelines is still doubtful when it comes to slender bridge piers.

This dissertation includes the analytical study done on twenty-seven slender bridge pier models to determine the extent of critical plastic and cracked zone at the base . Nonlinear static analysis is performed in the present study in which the pier is subjected to lateral deformation along with axial force applied simultaneously using MIDAS FEA software package both without incremental load steps and with five incremental load steps. The effect of variation in percentage of longitudinal reinforcement, shear reinforcement and axial load ratio on the plastic and the cracked zone is studied, keeping the cross section of pier and the grade of steel and concrete same for all the models.

The results obtained after analysis e.g. height of fully open , partially open cracked zone and the height of plastic zone are graphically represented and the effect of one of the factors on these heights keeping other two factors constant is studied. Also, the length up to which the lateral confinement required for ductility demand of bridge piers is determined based on the height of plastic zone obtained for each model and the same is compared with existing international codal provisions. It was observed that the maximum height of plastic zone obtained in the present study is more than the maximum height of lateral confinement suggested by various international guidelines. This observation indicates that the current codal provisions for height of lateral confinement are not fully reliable for slender bridge piers and hence these guidelines need to be revised after more detailed and diagnostic study.

Keywords: Plastic region length, lateral confinement, non-linear static analysis, slender pier ductility, Finite Element Analysis.

# TABLE OF CONTENTS

# LIST OF TABLES

**S.No** **Table Details** **Page No**

# LIST OF FIGURES

**S.No** **Figure Details** **Page No**

# LIST OF SYMBOLS

| Symbol | Symbol Details |
|---|---|
| $\alpha$ | Strain In Thorenfeldt Compression Curve |
| $\alpha_p$ | Peak Strain Value In Thorenfeldt Compression Curve |
| D | Depth From Extreme Compression Fiber To Tension Steel |
| $\varepsilon_c$ | Strain In Extreme Compression Fiber |
| $\varepsilon_s$ | Strain In Tension Steel |
| $\varepsilon_y$ | Yield Strain In Steel |
| $\varepsilon_{cu}$ | Ultimate Compressive Strain |
| f | Stress In Thorenfeldt Compression Curve |
| $f_t$ | Tensile Strength |
| $f_c$ | Uniaxial Strength. |
| $f_p$ | Peak Stress Value In Thorenfeldt Compression Curve |
| $G^I_f$ | Tensile fracture energy |
| h | Crack band width |
| $k_d$ | Neutral Axis Depth |
| K | Yield Stress Under Pure Shear |
| $L_{pr}$ | Plastic Region Length |
| $L_p$ | Analytical Plastic Hinge Length |
| $L_o$ | Length Of The Special Detailing Zone |
| M-Φ | Moment Curvature Relationships |
| $M_{NL}$ | Non-Linear Moment Profile |
| $M_L$ | Linear Moment Profile |
| P-δ | Second Order Non Linear Moment Effects |
| P-Δ | Load –Deformation |
| $\phi$ | Curvature |
| $\phi_u$ | Ultimate Curvature |
| $\phi_y$ | Curvature At Yield |
| $\phi_u/\phi_y$ | Curvature Ductility |
| R | Radius Of Curvature |
| s | Tie Spacing |

| | |
|---|---|
| $\tau_{oct}$ | Octahedral Shear Stress |
| $\rho_s$ | Percentage Of Longitudinal Steel |
| $\rho_{sh}$ | Percentage By Volume Of Lateral Steel |

# CHAPTER 1
# INTRODUCTION

## 1.1 GENERAL

Bridges play a very important role in every transportation network. When lateral forces are considered, the performance of a bridge relies predominantly on the piers that support the superstructure. This further requires the supporting piers to behave in such a way that the purpose of the bridge is fulfilled at all times of service while it may be subjected to various forces including uncertain lateral or seismic forces. This behavior of bridge columns can be ensured by imparting adequate ductility as the design philosophy for seismic analysis is primarily governed by ductility and the seismic energy is dissipated by post elastic deformation with the formation of flexural hinges at the pier base. This is very different when compared with the buildings where most of the energy of seismic forces is dissipated by formation of hinges in the beams while expecting the columns not to fail. This theory in building design is commonly referred as weak beam strong column theory. During the post elastic stage, it is also required that the pier possess sufficient strength to withstand the forces transferred by the superstructure to avoid failure of the entire system. However, in recent years the investigation and studies on bridge piers, that failed to provide sufficient strength after strong earthquakes, have indicated that despite undergoing energy dissipation by deforming in the inelastic region, failure in shear was responsible for the major damage. The deformations in the inelastic region that are often associated with the damage to the column, mostly concentrate at the junctions in the end where moment demands are maximum.

Apart from factors like low strength of material or poor-quality control, inadequate and insufficient detailing of reinforcement in bridges designed before 1980 was responsible for the failure of many piers. Damages due to excessive deformation in the inelastic region leads to cracking and finally spalling of concrete, which further propagates the failure. The spalling of concrete can be restricted or prolonged by properly confining the concrete using transverse ties or links placed at suitable locations where inelastic deformations are maximum ( usually ends of piers , with high moment demand) at adequate spacing. Hence the degree of confinement is a function of size, shape and spacing of the lateral reinforcement. The concept of formation and location of plastic hinges and critical plastic region must be ascertained so that confinement can be effectively done in that region. In the past two decades experiments performed on scaled models of various column sections have indicated that it is the end regions (the pier- pier cap

junction or the pier- footing junction) where bending and shear cracks lead to the formation of plastic hinges when subjected to both axial and horizontal cyclic load (Figure 1.1).Although various codes have proposed certain guidelines that define the zone of lateral confinement but experiments and research in the past have shown that these guidelines are not fully reliable. This may be due to the fact that most of the guidelines that are proposed did not consider the interaction of various factors like spacing of links , grade of steel used , strength of concrete, height of pier or column , axial load on column and the effects of tension shift , moment gradient and strain penetration on spread of plasticity. Also, in the last decade advancements in computer-based programs and software have resulted in better visualization of moment curvature curves, P-Δ curves , pushover analysis etc. With these advancements many researchers have proposed analytical models and compared the same with experiments on scaled specimens. Authors like R.Park , M.Priestley , E.M.Hines etc. have also proposed equations for calculating the critical plastic region which includes the interaction of all important factors contributing to the plastic spread.

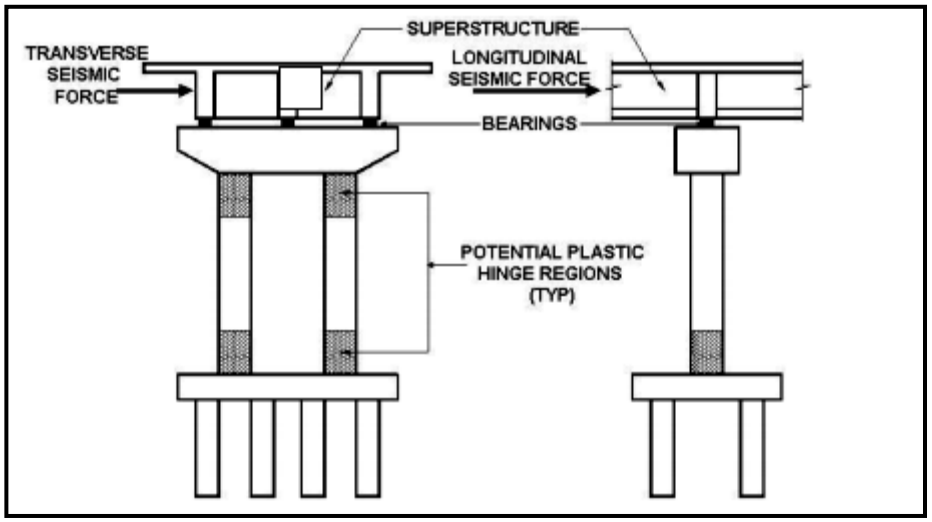


Figure 1.1 Potential Plastic Hinge Region (Tandon , 2005)

## 1.2 THEORY OF DUCTILITY

Ductility is a function of deformation characteristics of a member and is defined as the ratio of ultimate deformation of the member to the deformation at first yield. Ductility forms the basis of seismic design philosophy as most of the seismic energy is absorbed and dissipated by excessive post yield deformations. Generally, there are two approaches available with the designers to ensure adequate performance of the structure without undergoing any failure

whenever subjected to seismic forces. First approach is to design the structure for higher seismic forces than it will be subjected to as per the various earthquake zones of the region or design the structure to behave in a ductile manner.

The former approach is highly uneconomical and is seldom followed in practice while most of the designers go with the second approach that ensures ductile behavior of the structure. The load deformation graphs indicate a clearer inspection into the ductility characteristics for any member and are further dependent on moment curvature characteristics. This is true as most of the member deformations under normal proportions directly arise from flexure generated strains.

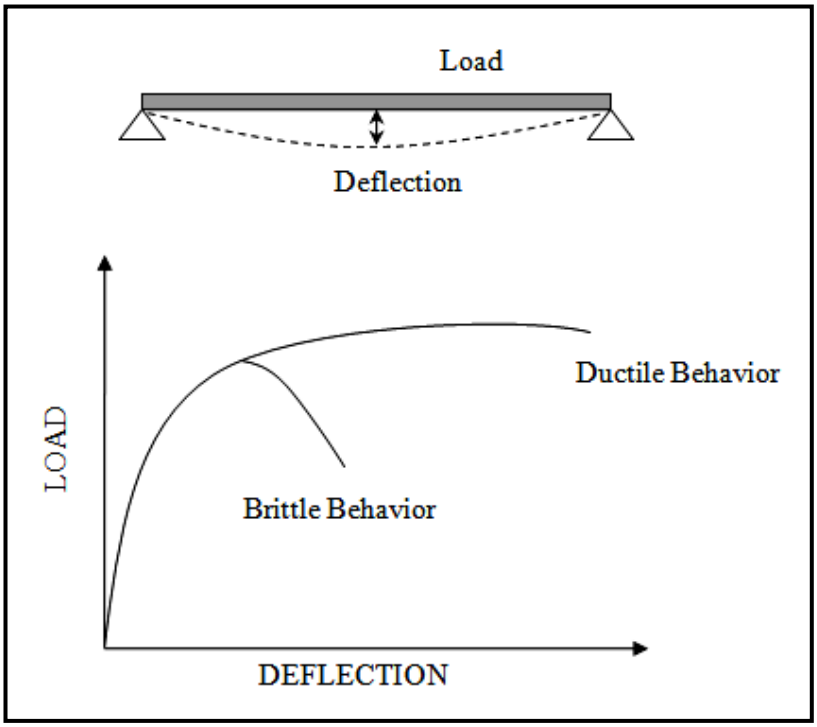


Figure 1.2 Load Deflection Curve ( Park et al ,1975 )

### 1.2.1 Moment curvature relationships

Curvature ($\phi$) of a member is defined as the gradient of strain profile at the element and is a function of neutral axis depth (kd), strain in concrete at extreme compression fibre , and strain in tension steel. It is generally the reciprocal of radius of curvature (R).Since at every section the strains are different and neutral axis depth also varies along the length, the curvature also varies along the length.

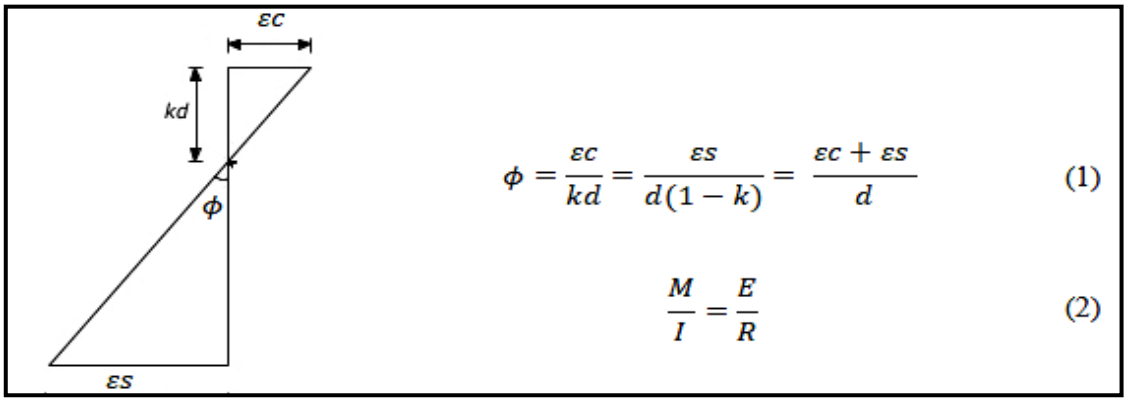


$$\phi = \frac{\varepsilon c}{kd} = \frac{\varepsilon s}{d(1-k)} = \frac{\varepsilon c + \varepsilon s}{d} \quad (1)$$

$$\frac{M}{I} = \frac{E}{R} \quad (2)$$

Figure 1.3 Strain Profile for a Loaded Beam ( Park et al ,1975 )

The relationship between moment (M) and curvature ($\phi$) as indicated by Equation (1) and Equation (2) can be wriiten as

$$M = I\frac{E}{R} = IE\phi \quad (3)$$

*1.2.1.1 Moment Curvature graph for beams*

When a beam member is subjected to loads , first crack (very minute) is developed while the stress range still lies in the initial portion of the stress strain curve .This is considered as the first stage with the moment curvature plot being linear and follows the trend as given by the equation. After the initial minute crack is developed, the amount of steel present in the section greatly influences the behavior of the section and the moment curvature relationship. Hence different nature of moment curvature graphs (Figure 1.4) for beams failing in tension or lightly reinforced beams and those failing in compression or heavily reinforced beams is observed.

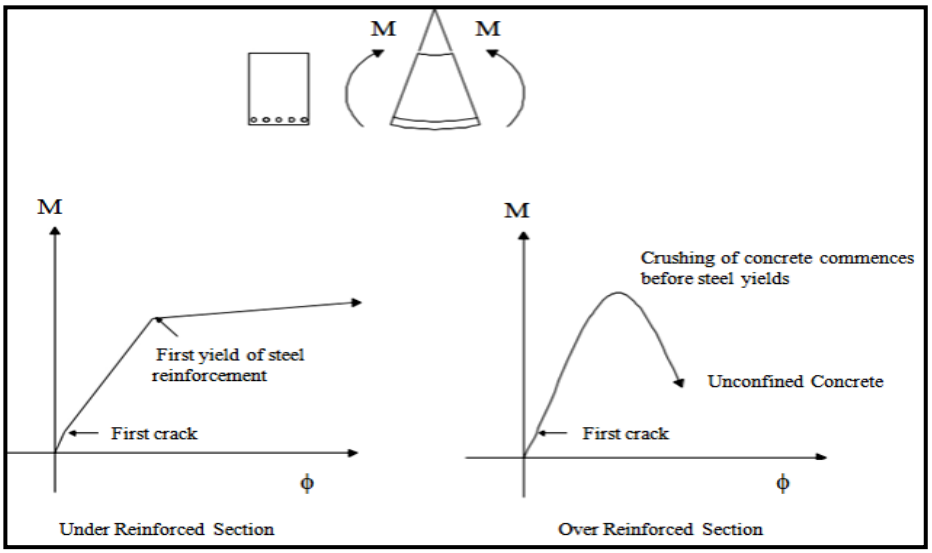


Figure 1.4 M-Φ Curves for RCC Beam Section ( Park et al ,1975 )

As the loads are increased and hence the bending moment enhanced , cracks start developing in the section which greatly reduce the flexural rigidity of the section. For lightly reinforced section this reduction in flexural rigidity is more as compared to a heavily reinforced section. The reason for this variation in reduction of flexural rigidity for differently reinforced sections is that a heavily reinforced section fails in a brittle manner and undergoes less deformation unlike a lightly reinforced beam which fails in a gradual manner undergoing larger deformations which further enhance cracks before actual failure. Thus, with large cracks the moment of inertia of the member also reduces resulting in a heavy loss of flexural rigidity. Figure 1.4 compares the nature of M-Φ graphs for heavily and lightly reinforced sections.

For a lightly reinforced beam, a practically linear M-Φ graph is obtained till steel starts yielding. Just when steel yields, the value of curvature increases by a large amount at nearly constant bending moment. Contrary to this for heavily reinforced section, after the first yield the relationship is non-linear as concrete enters the inelastic part of the stress strain curve. Also, if the section is not confined, the concrete crushes at relatively small curvature before the yielding of steel resulting in large reduction in the moment capacity and an early brittle failure. On the other hand, if the concrete is properly confined by closely spaced stirrups the section can undergo some more deformation before final failure. This comparison also validates the preference of under reinforced sections in routine design work ensuring a ductile behavior of the section.

The curvature ductility is given by the ratio of curvature at failure i.e ultimate curvature (Φu) to curvature at yield (Φy) indicated by following equations.

$$\phi_u = \frac{\varepsilon_{cu}}{kd} \tag{4}$$

$$\phi_y = \frac{\varepsilon_y}{d - kd} \tag{5}$$

$$Curvature\ Ductility = \frac{\phi_u}{\phi_y} \tag{6}$$

The influence of amount of reinforcement in the section on M-Φ graphs also direct us to draw many conclusions regarding ductility of the member.

- With the increase in tension steel content for an unconfined concrete section, the capacity to undergo large deformations is less indicating a decrease in ductility. This can also be confirmed by Equation (5) for curvature. With more steel content the depth

of neutral axis increases and as per the basic equation for curvature, the yield curvature Φy increases and the curvature ductility (Φu /Φy) decreases.

- If steel in compression zone is present, then the critical strain in concrete is taken care by compression steel along with the unconfined concrete which allows more deformation and hence an increase in ductility.
- Increasing the grade of concrete significantly enhances the ductility characteristics of section.
- Increase in the yield strength of steel also decreases curvature ductility because a higher grade of steel has higher yield strain resulting in higher yield curvature thus reducing the overall ratio (Φu /Φy).

*1.2.1.2 Moment Curvature graph for unconfined columns*

Unlike beams which are primarily subjected to transverse loads, the M-Φ graphs can be plotted with good efficiency and the deformation characteristics of the member can be determined with reasonable accuracy. However, for a column section, axial load also influences the curvature and thus for a given column section no unique curve for moment curvature exists. But for a given interaction curve corresponding graph for curvature can be plotted.

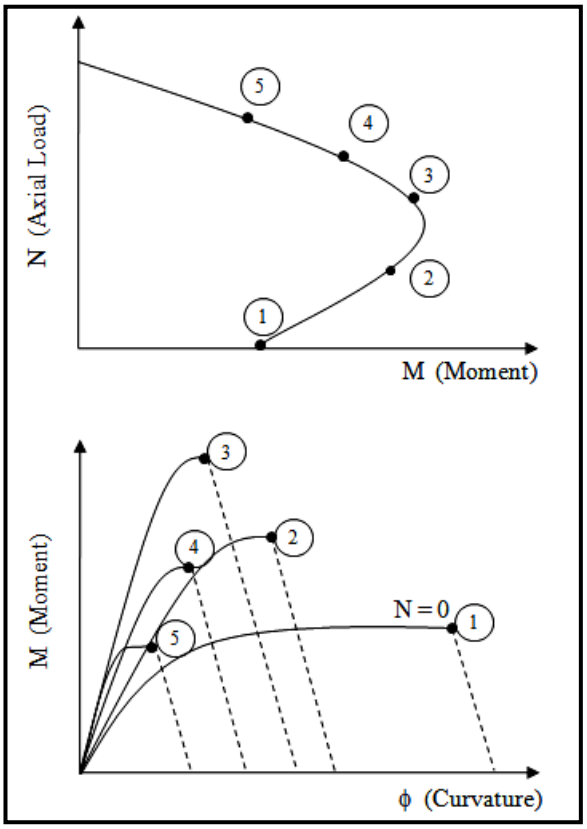


Figure 1.5 M-ϕ Curve Corresponding to Interaction Curve for Column ( Park et al ,1975 )

## 1.3 CURRENT SEISMIC DESIGN GUIDELINES

Seismic design guidelines require special detailing and enhanced confinement steel reinforcement in the plastic regions of RC columns to ensure stable ductile response. Following are the required guidelines for the confinement detailing as per various codes.

### 1.3.1 ACI-318-11

Building Code Requirements for Structural Concrete (ACI 318-11) is published by American Concrete Institute. This code covers the materials of structural concrete , the design aspects and the construction specifications that are used in buildings. In non-building structures too the guidelines mentioned in this code can be referred where applicable. The evaluation of strength of existing concrete structures is also covered in this code.

As per this code the length of the critical region in columns of ductile moment frames is the larger of:

- maximum dimension of the cross section,
- one-sixth of the clear span or
- 450 mm.

### 1.3.2 Canadian standard (CAN/CSA-A23.3-04)

CAN/CSA-A23.3-04 is the national standard code of Canada that was approved in July 2007 by Canadian Standard Association (CSA).This code also includes various guidelines and provisions for the design of reinforced concrete structures in detail covering all components of structural engineering. According to this code, the length of the special detailing zone ($l_o$) required for confinement effectiveness in columns for axial load ratios less than 0.5 is the greater of

- 1.5 times the largest cross-section dimension, or
- one-sixth of the clear span length.

### 1.3.3 AASHTO

In United States , American Association of State Highway and Transportation Officials (AASHTO) sets up design guidelines for the construction of highways throughout the country.AASHTO bridge design specifications covers the design, evaluation and rehabilitation of highway bridges. The AASHTO seismic design guidelines define a plastic region length ($L_{pr}$) in bridge piers as the largest value of:

- 1.5 times the dimension of the cross section in the bending direction,
- The length of the region where the moment demand exceeds 75% of the maximum plastic moment, or
- The analytical plastic hinge length ($L_p$).

1.3.4 CALTRANS

The Seismic Design Centre (SDC) of California Department of Transportation (Caltrans) suggests certain basic minimum requirements which are considered important to ensure adequate performance for ordinary bridges whenever seismic activities occur. The SDC expects the ordinary bridges designed as per these specifications to at least remain standing despite some significant damage, rendering the bridge unserviceable whenever a Design Seismic Hazard occurs. According to the guidelines laid by CALTRANS, the length of the special detailing zone ($l_o$) required for confinement effectiveness in piers is the greater of :

- 1.5 times the dimension of the cross section in the bending direction,
- The length of the region where the moment demand exceeds 75% of the maximum plastic moment, or
- 1/4 times distance from the location of maximum moment to the point of contra-flexure.

1.3.5 New Zealand Standard (NZS 3101: 2007)

The New Zealand standard (NZS 3101:2007) lays down the guidelines regarding minimum requirements for safe and more reliable design of both reinforced concrete structures and prestressed concrete structures. Also, it enables the structural engineers to verify the compliance of concrete structures with another existing standard known by the name New Zealand Building Code. The seismic guidelines as per this code require the ductile detailing length in columns for effective confinement to be the greater of

- The dimension of the cross section in the direction of the resisting moment and
- The length of the region over which the design moment exceeds 80% of the end moment for axial load ratio < 0.25, which is often the maximum axial load level in bridge columns.

1.3.6 Eurocode 8 (EN 1998-2:2005)

EN 1998 Eurocode 8, in general is applicable to the design and construction of buildings and other civil engineering works in seismic regions. It contains 6 parts in total, out of which part

2 provides the guidelines for earthquake resistance design of bridges. As per this code, the lateral seismic actions are mainly tackled by allowing the piers or the abutments to bend. This code also enlists guidelines for the seismic design of cable stayed and arch buildings.

Clause 6.2.1.5 of this code specifies the extent of zone of lateral confinement based on axial load ratios and the same have been shown below.

(a) For axial load ratio up to 0.3, Length of plastic zone is taken to be maximum of :

- The dimension of the cross section in the plane of bending.
- The length of the region over which the design moment exceeds 80% of the end moment.

(b) For axial load ratio between 0.6 to 0.3, length of plastic zone is taken to be 50% more than that determined by criteria (a)

1.3.7 Code of Practice For Concrete Road Bridges. Indian Roads Congress (IRC 112:2011)

Indian Road Congress took an important step by combining the code for reinforced concrete and prestressed concrete for bridges into a single unified bridge code which is known as IRC 112:2011.This code follows limit state design philosophy and has significant improvements when compared with previous codes like IRC 21 and IRC 18.The improved method of reinforcement detailing in context to previous design practice in India is one of the key features of this code. When it comes to detailing of piers for effective confinement, this code enlists similar guidelines as prescribed by EN 1998-2:2005 above. For effective confinement, the guidelines for lateral reinforcement as per IRC:112-2011 are applicable only for bridges located in zones III, IV and V of seismic zone map given in IRC:6-2010.The length of zone of special confinement in piers as per this code is as follows.

(a) For axial load ratio up to 0.3, length of plastic zone is taken to be maximum of :

- The dimension of the cross section in the plane of bending.
- The length of the region over which the design moment exceeds 80% of the end moment.

(b) For axial load ratio between 0.6 to 0.3, length of plastic zone is taken to be 50% more than that determined by criteria (a)

(c) Confinement shall extend up to length where the value of the compressive strain exceeds

0.5 $\varepsilon_{cu2}$.

## 1.4 OBJECTIVES OF CURRENT DISSERTATION

The key objective of this dissertation was to take an industry-oriented research problem. One such problem encountered in the bridge design industry is the determination of exact height up to which lateral confinement in terms of closely spaced ties or hoops, be provided to impart and enhance sufficient ductility of the bridge piers .During seismic activities , it is expected that no plastic hinges are formed in the superstructure of the bridges and rather the seismic energy is dissipated by allowing deformations in the piers and at the same time preventing the immediate collapse of the piers and the bridge itself as a result of these excessive deformations.

Various international codes have prescribed certain guidelines and methods to determine the height from the base of the pier up to which this special confining reinforcement should be provided. However, these guidelines are prescribed in general without considering whether the pier is a short pier or a slender pier. Moreover, most of the previous research has focused on determination of length of plastic hinge at the base of the pier and the factors affecting it considering piers with slenderness ratio less than 10. As the slenderness ratio increases the nature of failure shifts from a shear failure to a flexure failure and also the second order effects i.e. P-δ effect also influence this zone of plastic hinge formation which actually enhances it. Hence there needs to be a clear classification of the height of zone of lateral confinement in the bridge piers depending on the slenderness ratio.

The objective of the present study is to validate the provisions prescribed by various international codes regarding the zone of lateral confinement for a solid slender bridge pier and study the effect of variation of factors like percentage of lateral reinforcement, percentage of longitudinal reinforcement and change in axial load ratio on fully open cracked zone and the height of plastic zone formed near the base of the pier.

## 1.5 ORGANISATION OF WORK

The work done for developing this dissertation report has been organized into five chapters. A brief description about these five chapters is shown in Table 1.1.

Chapter 1 describes the basic objective of the work done in this dissertation. It includes the problem taken for the dissertation and compares various existing practices followed in the bridge design industry as per existing international guidelines

Table 1.1 Organization of Work

| Chapter No | Name of the Chapter |
|---|---|
| 1 | Introduction |
| 2 | Literature Review |
| 3 | Methodology |
| 4 | Results and Discussions |
| 5 | Conclusions |

Chapter 1 describes the basic objective of the work done in this dissertation. It includes the problem taken for the dissertation and compares various existing practices followed in the bridge design industry as per existing international guidelines. It explains why slender piers were selected for the current work. Literature referred during this whole process of working on this dissertation, has been described briefly in Chapter 2. The effect of various factors like slenderness ratio, axial load ratio, grade of concrete and steel, percentage of lateral reinforcement etc. considered by different researchers all around the globe on the plastic zone developed in the piers has been briefly outlined in this chapter.

Chapter 3 explains the detailed approach adopted in the present study to determine the effect of factors considered in this work on the height of fully open cracked zone and the plastic zone of the slender pier models. It mentions the details of all twenty-seven models in terms of percentage of lateral and longitudinal reinforcement along with axial load ratio imposed on each of the model. The details of geometric modelling, meshing of the pier, load applications, boundary conditions, constitutive models used, iteration procedures adopted etc. are described in detail in this third chapter.

After performing finite element analysis on all the pier models, the results for both incremental and non-incremental loading are sorted and classified in fourth chapter. The graphical representation of the results has been done to study the effect of one factor on height of plastic zone and fully open cracked zone, keeping other two factors constant. The possible reasons for the observations made are also described in the same chapter. The comparison of length of zone of lateral confinement as per existing codal provisions of various international codes (as already explained in section 1.3) is also done in this chapter with the results obtained from the current analytical study.

In the final chapter, the conclusions drawn from the results obtained in chapter 4 are briefly described and the future scope of the present study is mentioned. The general observations

obtained from the analysis of these slender pier models have been described in this closing chapter.

# CHAPTER 2
# LITERATURE REVIEW

## 2.1 HISTORY

The severe damage caused by earthquakes to the bridge structures during 1970-1980 , indicated the urgent need of experimental and theoretical research regarding the seismic performance of bridges. Since then many researchers stepped forward to perform experiments on scaled models to understand the factors and their interaction on the performance of bridge piers. Investigation of damaged bridges also directed towards a ductile response of piers and thus most of the work of researchers focused on improvement of ductility of the bridge piers by variation in reinforcement pattern, spacing of ties , confining the zone of critical plastic region etc. Agencies like CALTRANS also funded many universities and researchers so that better guidelines could be framed making use of the experimental results. Also, with the advancement in computer technology many researchers generated analytical models and proposed certain equations for determining the spread of plasticity. This section discusses and compares some of the research published in the areas of improvement in the performance of bridge piers when subjected to lateral ground motion and includes both analytical models and experimental work.

## 2.2 EFFECT OF SLENDERNESS ON DUCTILITY & PLASTIC ZONE LENGTH

**Babazadeh et al. (2016)** discussed the effect of slenderness on critical plastic region $L_{pr}$ and aimed to evaluate the components of critical plastic region.

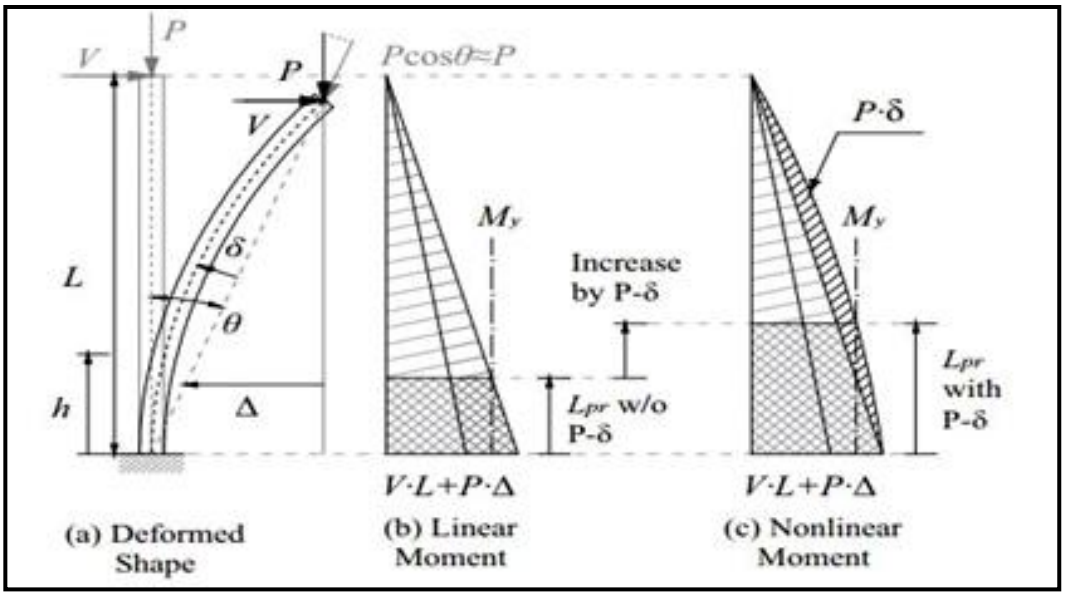


Figure 2.1 Effect of P-δ Moments on Plastic Spread ( Babazadeh et al , 2016)

His work mainly focused on determining the effect of nonlinear moment, ($M_{NL}$) profile due to P-δ effect on the spread of plastic region. He compared the existing current seismic design guidelines suggested by ACI code (ACI-318-11), Eurocode 8 for buildings (EN 1998-1:2004) Canadian standard (CAN/CSA-A23.3-04), AASHTO and Caltrans and concluded that all guidelines except those framed by Caltrans , underestimated the length of critical plastic zone.

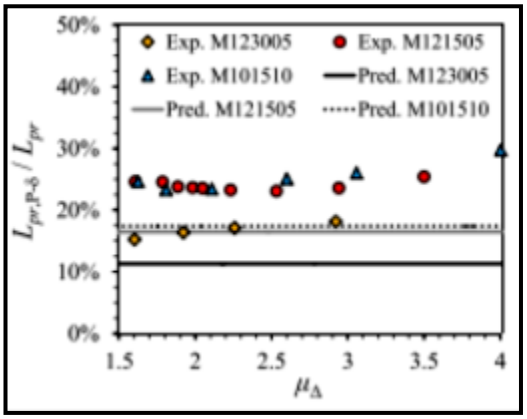


Figure 2.2 Experimental and Model Results Comparison for P-δ Effect.( Babazadeh et al , 2016)

The effects of slenderness and the associated member flexibility on $L_{pr}$ were assessed through the contribution of P-δ moments ($L_{pr}$, P-δ). Comparison of the results obtained from linear ($M_L$) and nonlinear ($M_{NL}$) moment profiles demonstrated the increase of the plastic region due to P-δ effects. Therefore, $L_{pr}$, P-δ was experimentally determined according to ($L_{pr,NL}$ - $L_{pr,L}$). To illustrate the contribution of moment nonlinearity to the spread of plasticity, the ratio $L_{pr,P-\delta}$ / $L_{pr}$ is plotted in Figure 2.2 and Figure 2.3. It can be seen that, on average, P-δ moments account for 20% of the total $L_{pr}$.

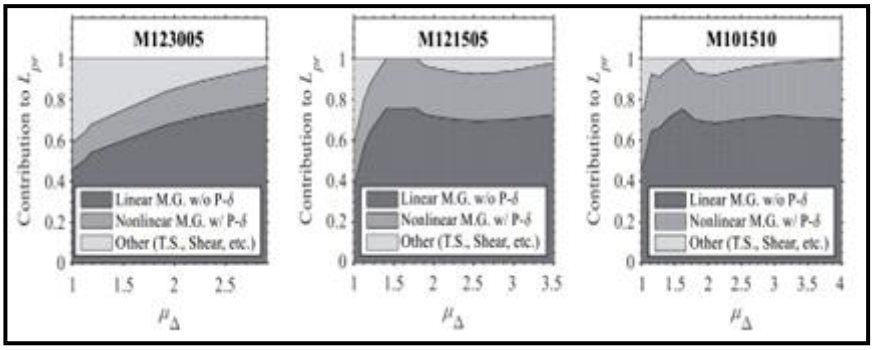


Figure 2.3 Contribution of P-δ Effect to Plastic Spread ( Babazadeh et al , 2016)

**Reza et al. (2014)** performed a detailed pushover analysis to determine the effect of short , intermediate and long piers on ductility, by varying the slenderness ratio as 2.4, 4.8 and 7.2.Although all these ratios are less than 12, indicating that these piers belong to the category of short piers only, but when compared against each other, pier with ratio 7.2 is more slender

than other two piers and similarly pier with ratio 4.8 is more slender than the pier with ratio 2.4.For each column height 81 models were analyzed based on various factors taken in their study. Lateral load was applied in the shorter dimension of the column cross section. The pushover deformation shape of column and the cross section adopted is shown below. The height was varied as 7m, 14m and 21m keeping the cross section same to maintain the slenderness ratio as described above.

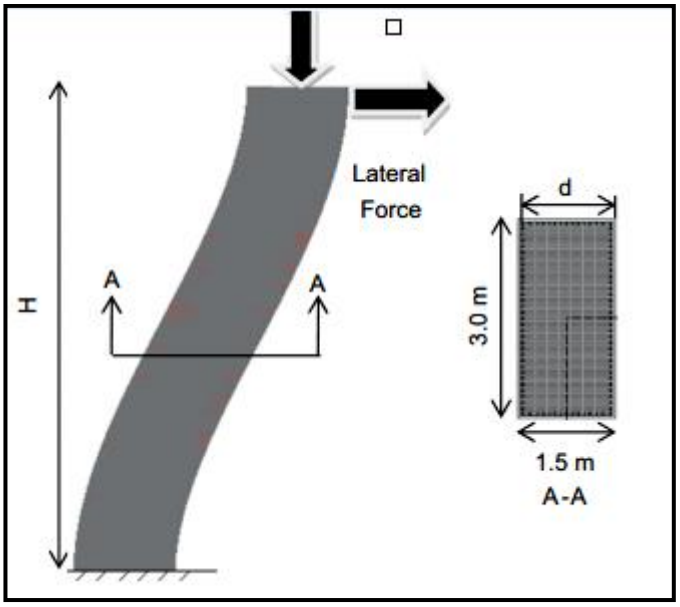


Figure 2.4 Pushover Deformation Shape of Column along with Cross Section Details ( Reza et al., 2014)

It was observed that column with the lowest slenderness ratio was mostly shear dominated and as the slenderness ratio increased with the increase in the height of the column due to uniform cross section, a shift from shear dominance to flexure dominance was witnessed. Columns which failed in flexure and not in shear were seen to have very less influence of lateral confinement before yielding occurred. However, after yielding the effect of lateral confinement was significant on the crushing displacement and ductility, especially for columns with lesser slenderness ratio.

For column with height 7 m, out of 81 models, 45 models were shear dominated. Out of these 45 models,39 models were observed to have displacement at shear failure lesser than the yield displacement i.e indicating ductility less than 1.Only one out of these 45 models had ductility ratio 2.43.The variation in ductility with the height of column for all 81 models per height, is indicated in Figure 2.5.Also, it was observed that the range in ductility is more for column with height equal to 14m indicating that ductility does not follow a common trend as the height of the columns is increased.

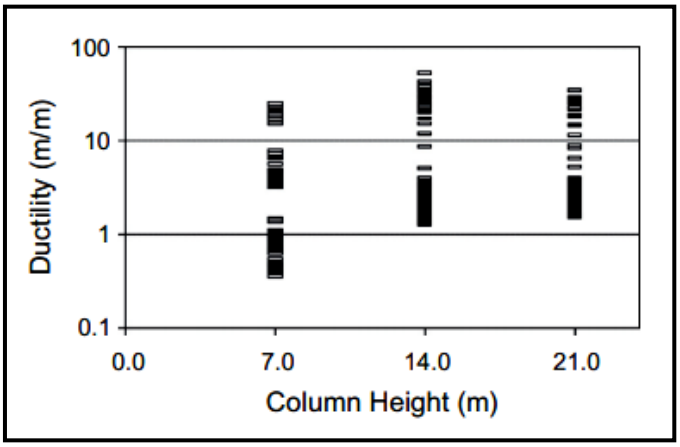


Figure 2.5 Range of Ductility with Different Heights of Column ( Reza et al.,2014)

**Cassese et al. (2017)** performed experimental tests on scaled models of a typically existing reinforced concrete bridge pier with a hollow rectangular cross section. A total of four specimens were tested with different ratios of slenderness. Displacement controlled loading was applied along with a constant axial load on all the four specimens. These specimens were detailed in such a way so as to represent typical design practices prevalent before 1980s. Low percentage of longitudinal and lateral steel was provided in all these specimens without any provision of confinement steel. It was observed after the experiments that two types of failure modes were prevalent. For piers with greater slenderness ratio , flexure type failure was witnessed and for piers with lower slenderness ratios, flexure-shear type of failure was noted. Following table shows the details of the four test specimens along with the failure modes reported by the authors.

Table 2.1 Details of Test Specimen (Cassese et al.2017)

| Test Specimen Id | Slenderness Ratio | Modes of failure reported |
|---|---|---|
| P1 | 2.50 | Flexure |
| P2 | 3.75 | Flexure |
| P3 | 1.50 | Shear |
| P4 | 2.25 | Flexure-Shear |

The authors reported that the tests specimens having higher slenderness ratio i.e. P1 and P2, which had flexural mode of failure showed a ductile mechanism in response to loading in the inelastic stage. The type of damage (Figure 2.6) corresponded to that of a typical ductile member and was characterized by spalling and crushing of concrete and buckling of main reinforcement bars.

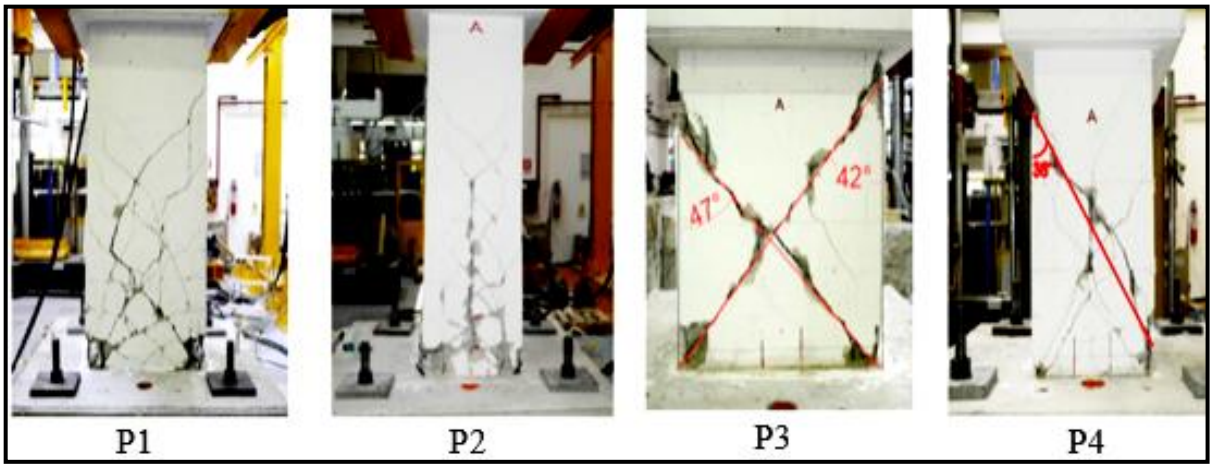


Figure 2.6 Final Damage State of Specimens Depicting Mode of Failure (Cassese et al.,2017)

Test specimen P3 which had the lowest aspect ratio, failed in shear after yielding in flexure. Appreciable diagonal cracking was reported during the testing which was inclined nearly around 42-47 degrees as can be seen in Figure 2.6.Test specimen P4 also showed shear failure after flexural yielding but during the non-linear phase, the damage propagated by flexural cracks near the base which were then succeeded by significant diagonal cracks up to final shear failure. However, the angle of final shear crack was less ( 30 degree) in comparison to the test specimen P3.These results indicate that flexure failure is predominant in piers with higher slenderness ratio which further influences the plastic zone also.

## 2.3 EFFECT OF AXIAL LOAD RATIO ON CURVATURE DUCTILITY

**Zahn et al. (1986)** performed experimental studies on large range of RCC columns for developing design charts and design procedures for the flexural strength and ductility of such members based on cyclic moment curvature graphs that were plotted using cyclic stress strain curves for steel and concrete for Ministry of Works and Development (MWD).

In their study the authors considered the deterioration of flexural strength of columns when subjected to high axial compression loads along with cyclic lateral loading. It can be seen from the following graph that the curvature ductility is higher for low axial load ratios. One of the major conclusions of their study was there is a substantial increase in the flexural strength of columns due to confinement of the concrete for axial compression load ratio greater than 0.3 . For smaller compression loads this increase is negligible for typical amounts of confining steel.

**Park et al. (1975)** also performed studies on many confined and unconfined sections to determine the effect of axial load ratios and found that for higher axial loads the ductility is considerably low as can be seen from Figure 2.8.

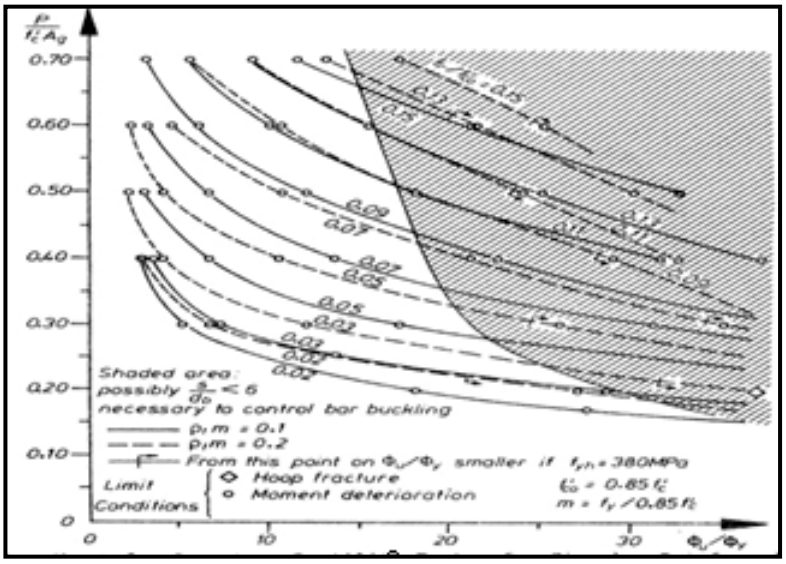


Figure 2.7 Design Chart for Curvature Ductility Factor for Circular RCC Column Sections.( Zahn et al. 1986)

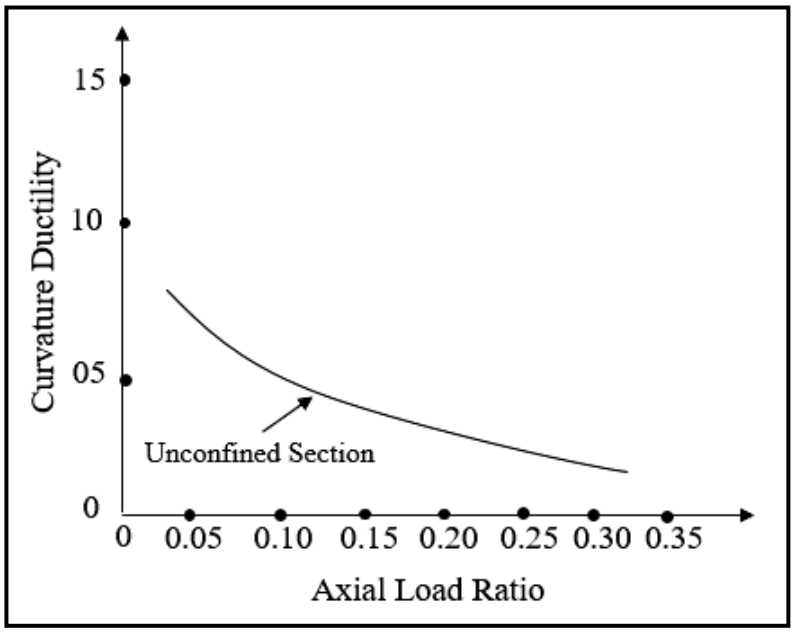


Figure 2.8 Effect of Axial Load Ratio on Curvature Ductility ( Park et al ,1975)

**Dowell et al. (2002)** developed plastic hinge length equations specifically for piers with non-conventional cross section geometries. While formulating the equation based on observations made from test results, they concluded that axial load ratio indirectly influences the length of plastic hinge length by changing the idealized moment curvature response of the section.

**Hines et al. (2004)** worked on developing an approach to estimate the horizontal force displacement response of well confined reinforced concrete bridge pier with particular emphasis on hollow rectangular piers. In their study the authors proposed an analytical model to derive spread of plasticity for axial load ratios upto 0.20 and also discussed the influence of tension shift. It was observed that the curvature ductility decreased with increasing axial load ratios.

**Matsui et al. (2000)** studied the effects of axial force on deformation capacity of steel encased reinforced concrete beam-columns by performing analytical research.The results indicated a maximum limit of axial force to ensure stable behavior of a steel encased reinforced concrete beam-column when it was subjected to both axial and repeated lateral loading.The maximum axial force that the beam-column can resist under cyclic lateral loading was defined as stable limit axial force to ensure the required rotation angle amplitude. Analytical results indicated that the stable limit axial load ratio increases as steel strength increases or compressive strength of concrete decreases and the curvature ductility decreases.

## 2.4 EFFECT OF CONFINEMENT ON DUCTILITY

**Priestley et al. (1977)** performed experimental studies on five pier units scaled to suitable size as shown in Table 1 to provide experimental results concerning code provisions for seismic design of bridge piers subjected to reversed flexure and axial loads. These test units represented variations of a prototype octagonal pier that was designed as per New Zealand seismic design requirements. Units 1 to 3 contained transverse reinforcement as per ACI provisions and differed only in the manner of their load application. Vertical reinforcement for units 1 to 3 was kept similar.

Table 2.2 Details of Test Units (Priestley et al. 1977)

| Unit | Scale | Vertical reinforcement | Hoop steel as per | Hoop steel | Load |
|---|---|---|---|---|---|
| 1 | 1/3 | 20 bundles of 2- 13ϕbars | ACI guidelines | 6.5 ϕ @ 65 mm | Static horizontal and vertical |
| 2 | 1/3 | 20 bundles of 2- 13ϕbars | ACI guidelines | 6.5 ϕ @ 65 mm | Static horizontal and vertical |
| 3 | 1/3 | 20 bundles of 2- 13ϕbars | ACI guidelines | 6.5 ϕ @ 65 mm | Static horizontal and vertical |
| 4 | 1/2 | 20 bundles of 2-13ϕbars | NZ guidelines | 8ϕ @ 34 mm | Static horizontal only |
| 5 | 1/6 | 10-13ϕ bars | NZ guidelines | 4.4ϕ @ 14 mm | Sinusoidal and earthquake base |

Unit 4 also contained same vertical reinforcement, but the transverse reinforcement was designed as per guidelines proposed by New Zealand highway bridge design brief. No vertical load was assigned to unit 4 and was subjected only to the horizontal load. Unit 5 consisted of different vertical reinforcement and also the scale was kept to be 1/6 of prototype. It was subjected to sinusoidal and earthquake base accelerations. The main objective of the author for

performing experiment on units 4 and 5 was to determine effect of scale and the response of units 4 and 5 due to change in test procedure. Moment  displacement response for the test units were plotted.

It was observed that unit 4 with the heavier transverse steel behaved exceptionally well. Stiffness degradation for unit 4 was minimum while unit 3 formed a substantial cavity inside the reinforcing cage. It was found that although adequate behavior was exhibited by all units, transverse steel as per ACI requirements for flexural members was not sufficient to restrain compression steel from buckling.

**Ro et al. (1992)** performed experiments on 10 column units with shear span to depth ratio 2.5 and the main bar ratio 1.0% subjected to axial and shear load.The authors presented in their study the relationships between shear loads and deflection angles which indicated that higher tie ratios , denser tie pitches are effective for higher ductility of the member at ends.

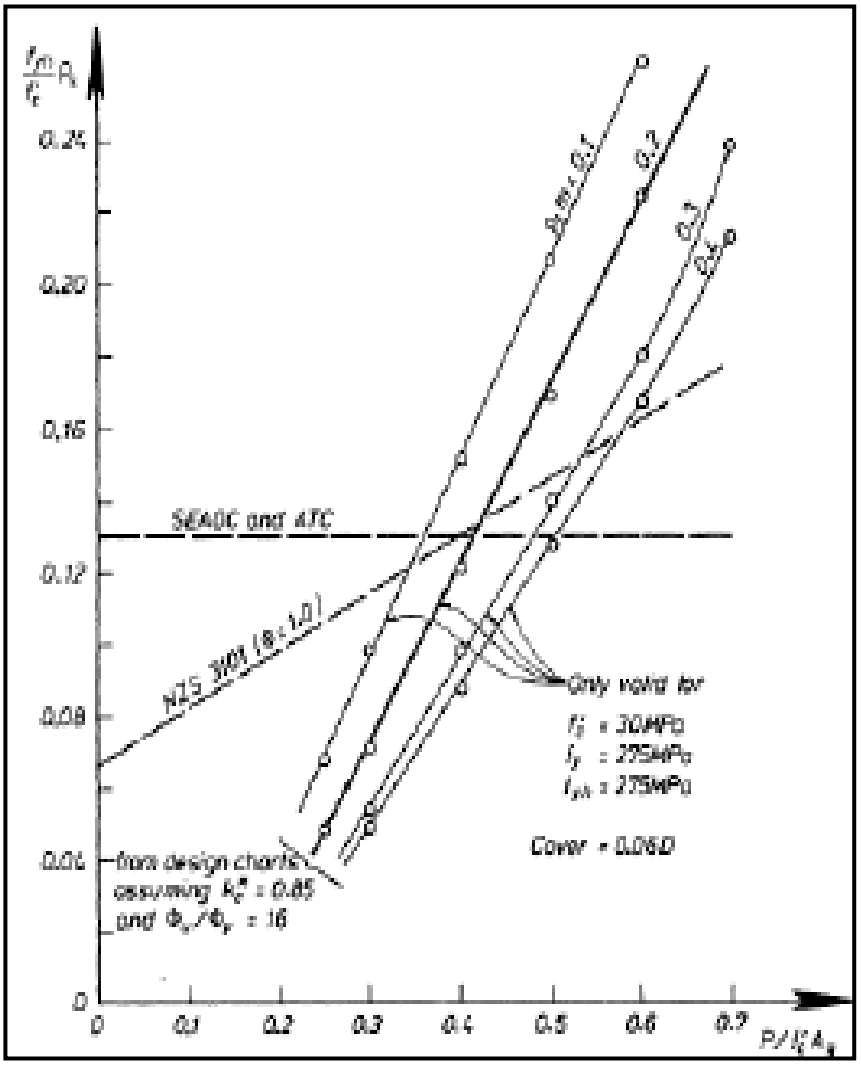


Figure 2.9 Design Chart for Calculating Tie Reinforcement (Priestley et al. 1977)

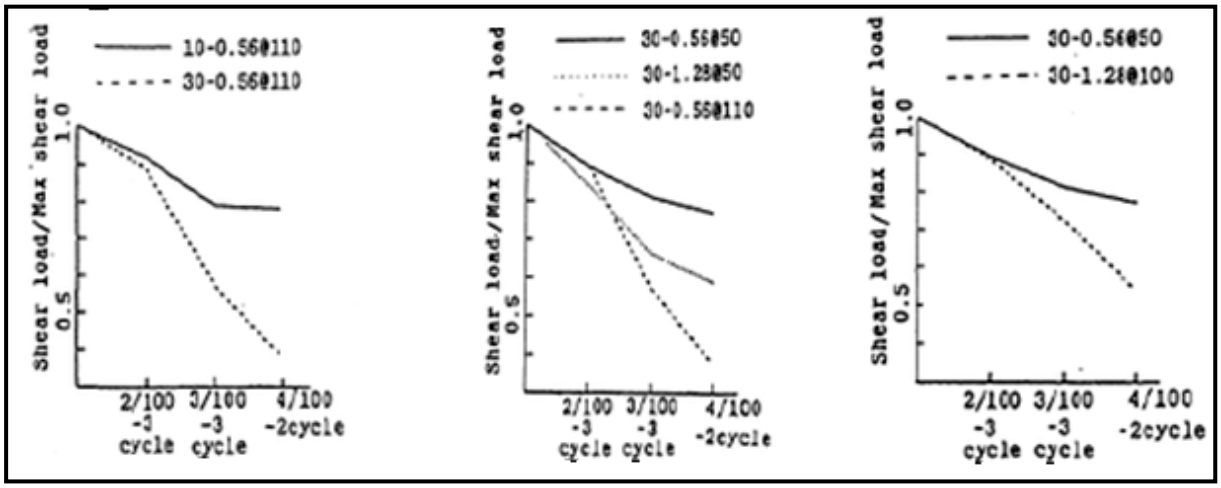


Figure 2.10 Shear Resistance for Different Tie Ratio and Tie Pitching (Ro et al. 1992)

**Maekawa et al. (2000)** developed an analytical model based on FEM and validated the same by performing experiments on a range of reinforced column sections. Their study aimed at determining the shear resistance and ductility of columns after yield of main reinforcement. Based on analytical simulation and experimental results a parametric study was conducted to determine the role of factors affecting the post yield deformability of reinforced concrete columns and a formula for ductility was proposed. The work in this study also helped in prediction of failure modes i.e. whether a shear failure(less shear span to depth ratio) will occur or a flexural failure will take place.

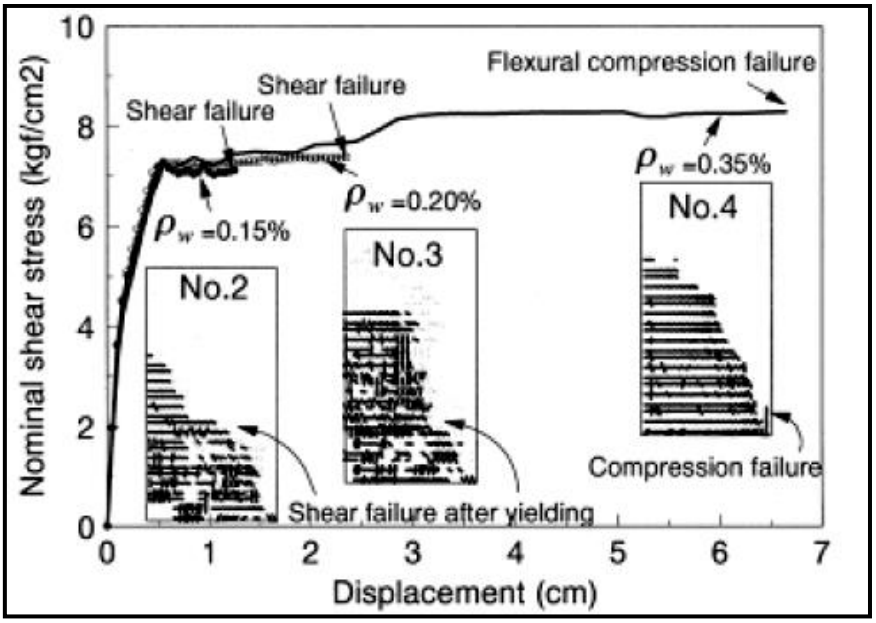


Figure 2.11 Effect of Web Reinforcement Ratio on Ductility of RCC Column ( Maekawa et al. 2000)

It was observed that the failure mode changes according to different amount of web reinforcement ratio from shear failure to flexural failure as the ratio increases. If the web

reinforcement is increased to 0.2% by volume, the shear capacity is increased but is still lower than two times the shear force at yield. Then, this case still brings shear failure, but higher ductility ratio can be expected. When the web reinforcement is increased to 0.35%, the shear capacity exceeds two times the shear force at yield. In this case, brittle shear failure may be avoidable, and the RC column may fail in flexure with high ductility.

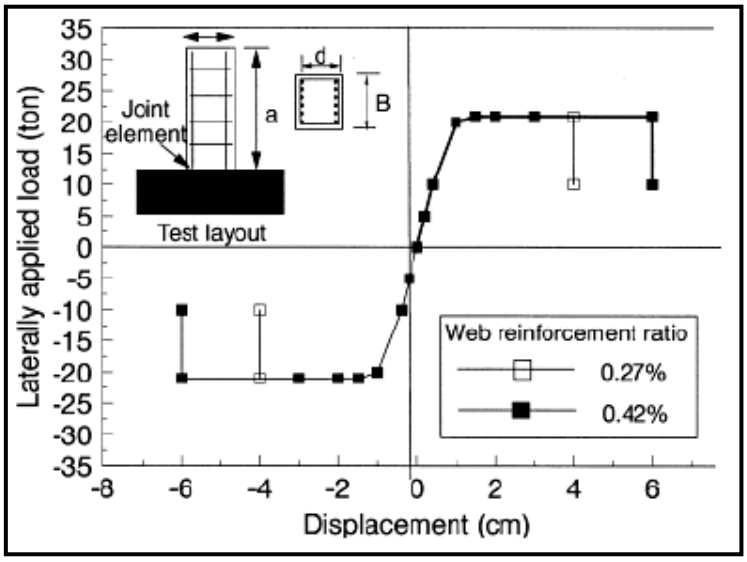


Figure 2.12 Envelope of Cyclic Load ± Displacement Relation of RCC Columns (Maekawa.et al. 2000)

The FEM simulation of ductility associated with shear failure was verified using the test data. The computational results indicate that an increase in web reinforcement ratio in the RC column yields higher ductility.

**Reza et al. (2014)** performed a detailed parametric study using factorial analysis to understand the effects of factors like tie spacing, concrete and steel properties, amount of reinforcement and column height and their interactions on limit states of bridge piers that can affect the performance of bridge piers under lateral loads. Compressive strength of concrete yield strength of steel, longitudinal steel reinforcement ratio and tie spacing were taken as the factors affecting the first cracking, yielding and crushing of 7 m, 14 m and 21 m height columns. The full factorial design of $3^4$ with no confounding patterns was conducted to observe the effect of different factors and their interactions among them. The three levels of these four factors are presented in Table 2.3**.** The effects estimated from these factorial analyses are valid for the ranges of factors mentioned in the table. Figure 2.13 shows the contribution of the four factors and their interactions on the base shear at cracking for different column heights. In this study, variations in three limit states: cracking, yielding of longitudinal bar and first crushing of concrete, with the change of four parameters (s, f'c , fy and $\rho_s$) have been investigated. .

Table 2.3 Factors for Factorial Analysis ( Reza et al. 2014)

| Factors | Low | Medium | High |
|---|---|---|---|
| Compressive strength of concrete | 25 | 40 | 60 |
| Yield strength of steel | 300 | 400 | 500 |
| Long steel ratio (%) | 2 | 3 | 4 |
| Tie Spacing (mm ) | 75 | 150 | 300 |
| Tie steel ratio (%) | 0.044 | 0.022 | 0.011 |

The results show that the compressive strength, longitudinal reinforcement and tie spacing have significant effect on the base shear at first cracking for 7 m height column. The effect of confinement of concrete on cracking base shear decreases with the increase in length of the column due to the increase of flexural dominance and decrease of shear dominance. Tie spacing has almost no effect on the yield base shear as shown in above figure. Figure 2.15 shows that the tie spacing has significant effect on the crushing base shear of 7 m column, however, very little effect for that of 14 and 21 m columns. In most of the cases, 7 m columns are shear critical and most of the combinations of 14 and 21 m columns are flexure dominated. The effect of tie spacing is insignificant on the base shear capacity of flexure dominated column, therefore, it has little effect on the crushing base shear for 14 and 21 m column cases as shown in Figure 2.15.

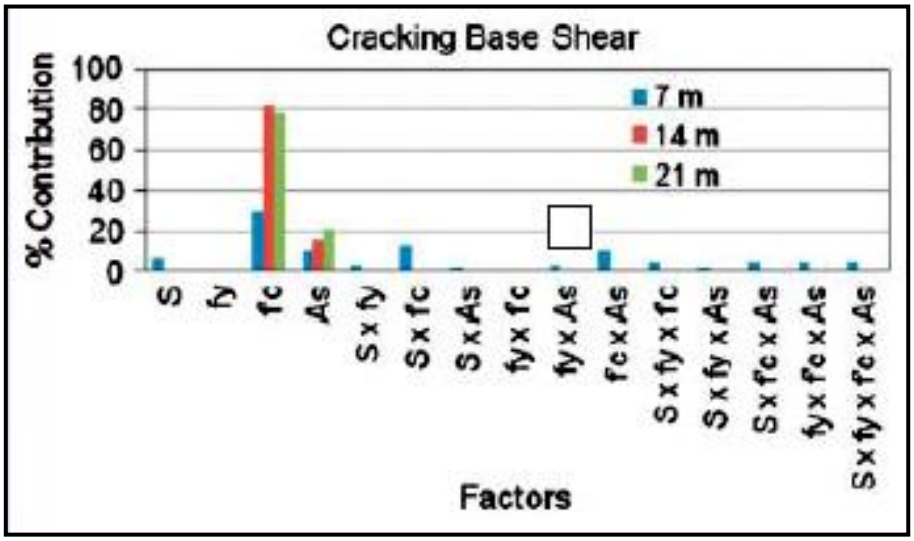


Figure 2.13 Contribution Percentage of Factors on the Change in Cracking Base Shear ( Reza et al. 2014)

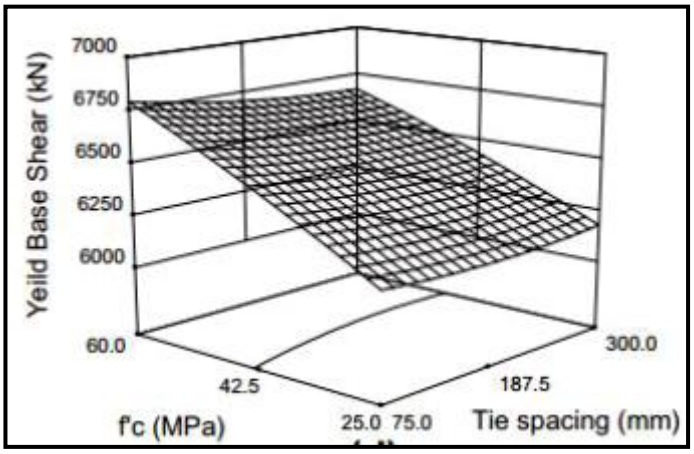


Figure 2.14 Effect of Tie Spacing and f'c ( Reza et al. 2014)

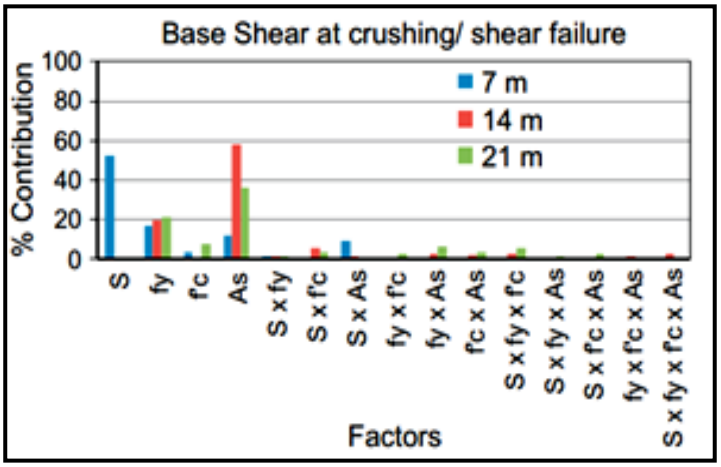


Figure 2.15 Contribution Percentage of Factors on the Change of Cracking Base Shear (Reza et al.2014)

The interaction between tie spacing and longitudinal reinforcement ratio is also significant as shown in Figure 2.16(b). The effect of tie spacing is higher for higher reinforcement ratio. Tie spacing, f'c and their interaction mostly affect the crushing displacement for the 7 m and 14 m height columns. Here, these two factors have significant interaction.

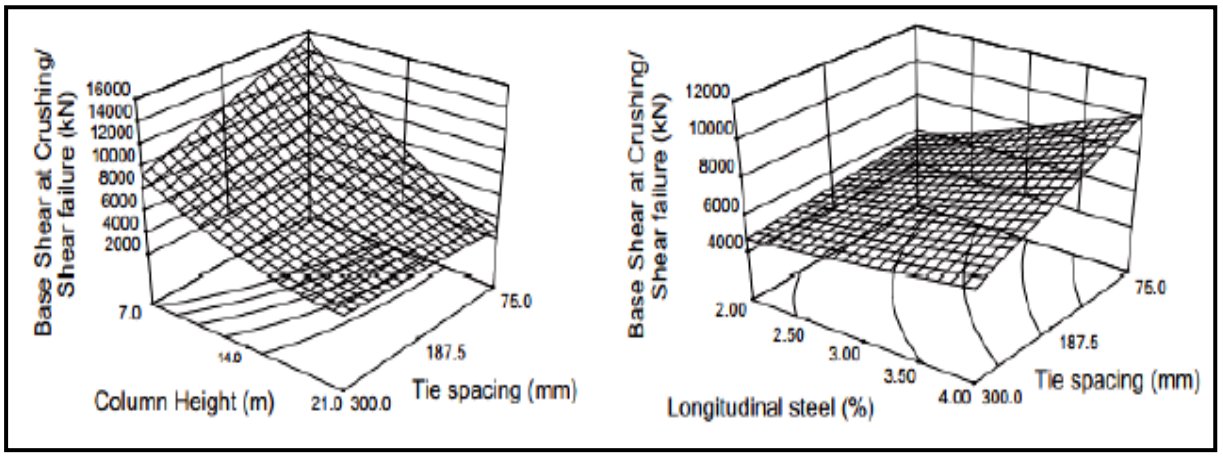


Figure 2.16 Effect of Column Height-Tie Spacing and Long Reinforcement Ratio-Tie Spacing (Reza et al.2014)

The effect of tie spacing decreases with the increase of column height from 7 m to 14 m and the effect of compressive strength increases. The effect of confinement becomes more significant after the first yielding. Tie spacing has higher effect on the displacement at crushing or shear failure for higher compressive strength of concrete. The percent contribution of tie spacing is higher in shorter column, however, the difference between highest and lowest displacements is smaller in shorter column (7 m column) than in longer column (14 and 21 m column). Therefore, crushing or shear failure displacement decreases with the increase of tie spacing for 14 and 21 m column, however, the effect of tie spacing is insignificant in the case of 7 m column as shown in Figure 2.17. The effects of tie spacing, f'c , column height, have been found significant on the ductility as shown in Figure 2.19. Figure 2.18 shows the interaction between tie spacing and f'c ; the effect of f'c is more for lower ties spacing.

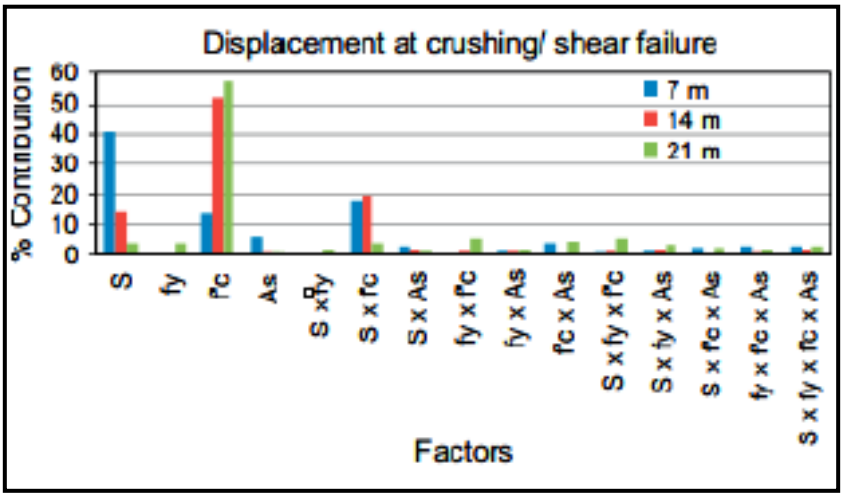


Figure 2.17 Contribution % of Factors on Displacement due to First Crush ( Reza et al. 2014)

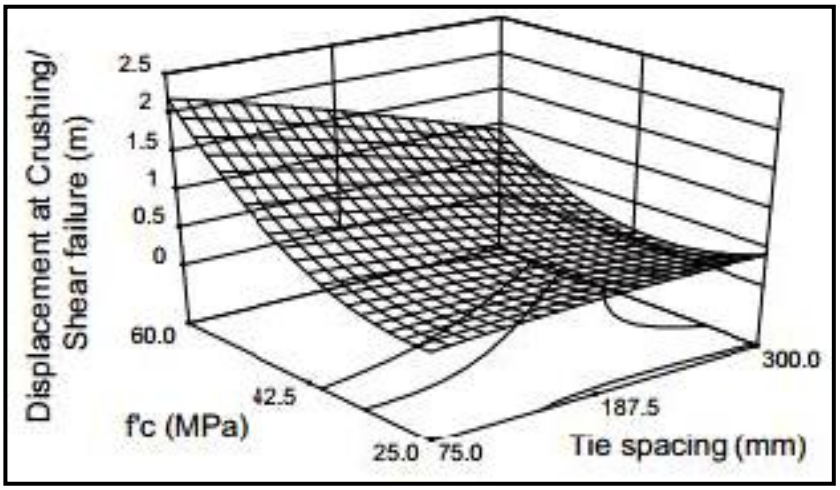


Figure 2.18 Effect of Tie Spacing and f'c,on Displacement at Crushing or Shear Failure (Reza et al. 2014)

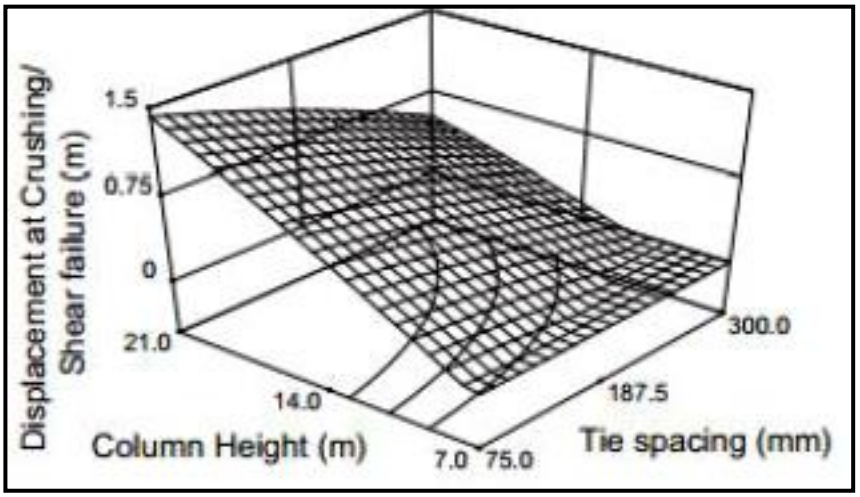


Figure 2.19 Effect of Column Height-Tie Spacing on Displacement at Crushing or Shear Failure (Reza et al. 2014)

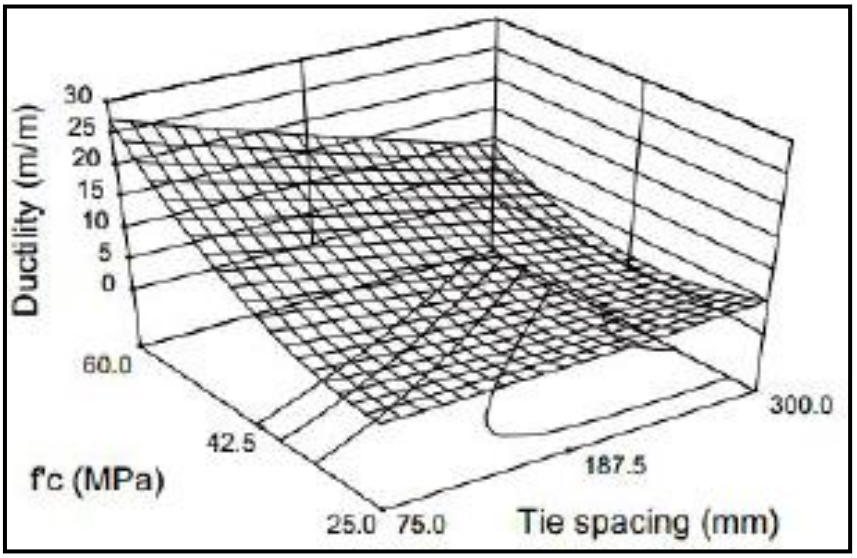


Figure 2.20 Effect of Tie Spacing and f'c on Ductility ( Reza et al.2014)

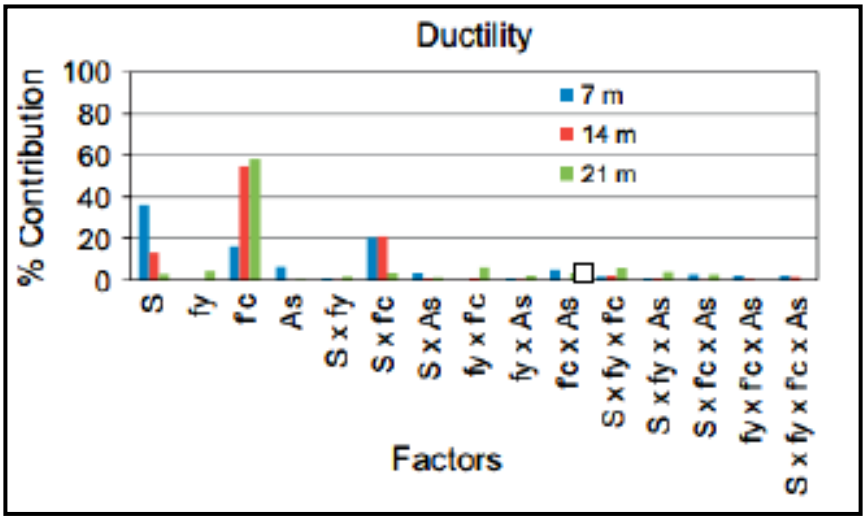


Figure 2.21 Contribution Percentage of Factors on Ductility ( Reza et al.2014)

2.4.1 Effect of tie shape on confinement effectiveness

**Kusuma et al. (2011)** compared experimental results with various analytical models available in the literature for the confinement of concrete by conventional rectilinear ties and welded wire fabric . The degree of confinement is related to the configuration, size and longitudinal spacing of the lateral reinforcement in the column. The study indicated that almost all the models are able to estimate correctly ascending part of stress-strain curve.

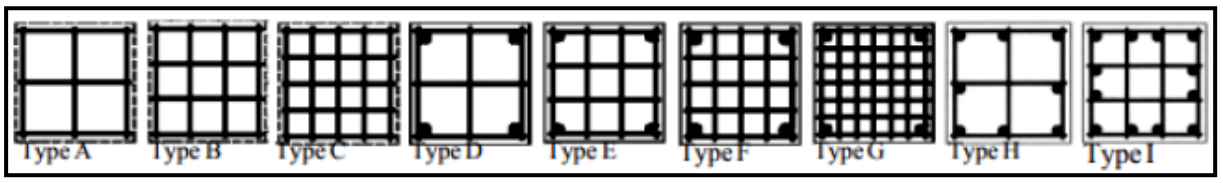


Figure 2.22 Arrangement of WWF (Kusuma et al. 2011)

However, there are wide variations in the prediction of the post-peak part of stress-strain curves, with a few models underestimating and overestimating the test behavior. Although none of the analytical models could accurately predict the full range of the experimental behavior, the predictions of the Akiyama et al. (2010) were generally in closest agreement with the experimental results.

**Papanikolaou et al. (2009)** performed a large parametric numerical analysis of solid and hollow reinforced concrete piers taken from actually constructed bridges, based on a consistent three-dimensional nonlinear finite element methodology. Various transverse reinforcement arrangements and spacing were examined, as well as the effect of high- strength concrete on confinement effectiveness.

Figure 2.23 shows the marginal difference in confinement effectiveness between spirals and circular hoops . A minor advantage of hoops is recorded due to their perfectly horizontal arrangement that coincides with the concrete expansion plane, as opposed to the slightly inclined spirals. The effectively confined region in the case of spirals appears asymmetric, especially for larger spacings (20 cm). Nevertheless, the use of spirals is preferred in practice, due to ease and speed of construction.

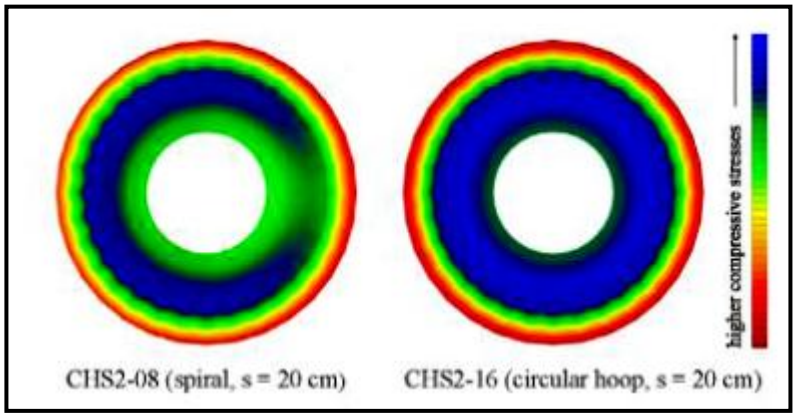


Figure 2.23 Contours of Axial Stresses at Ultimate Strength for the CHS2 Section with Spirals (left) and with Circular Hoops (right) (Papanikolaou et al , 2009)

In circular hollow sections, it was observed that the presence of an inner spiral (or hoop) does not significantly contribute to the strength and ductility of the confined section. Particularly in the thicker hollow section , the addition of an inner spiral led to reduced ductility, compared to the sole presence of an outer spiral.

A snapshot of the axial stress state (at ultimate strength) for this section (Figure 2.24) shows that the inner spiral unfavorably confines only the inner concrete cover, leaving an unconfined ring-shaped region around the inner spiral. As a result, the inner concrete cover tends to crack and spall off at high levels of axial strain (implosion), leading to the observed reduced ductility. This adverse effect can be referred as 'negative confinement'. Since there is generally no contribution in terms of strength and ductility from the use of inner transverse reinforcement, the respective economic indices suggest an uneconomical solution due to the larger steel volume required. Nevertheless, it is common practice, especially in Europe, to apply a sparsely spaced inner spiral in circular hollow sections, in order to control cracking due to environmental effects (serviceability limit state).

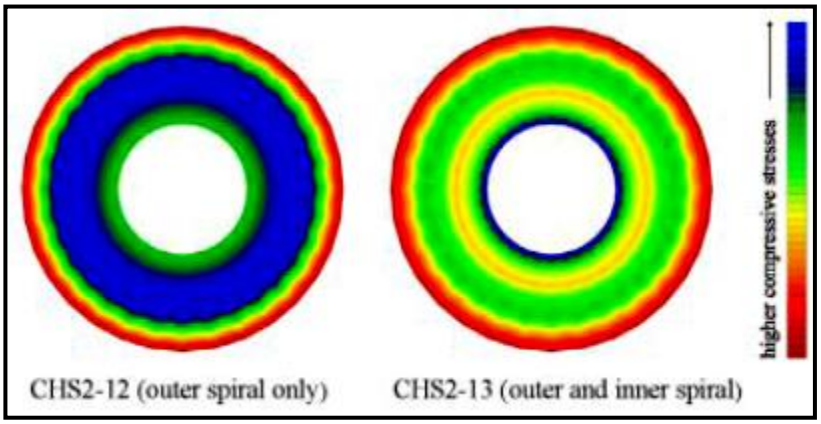


Figure 2.24 Contours of Axial Stresses at Ultimate Strength for The CHS2 Outer Spiral (left) and Outer and Inner Spiral (right) (Papanikolaou et al , 2009)

Notwithstanding the previous considerations, when the outer and inner spirals in hollow sections are effectively tied together using transverse links, both strength and ductility are substantially increased.

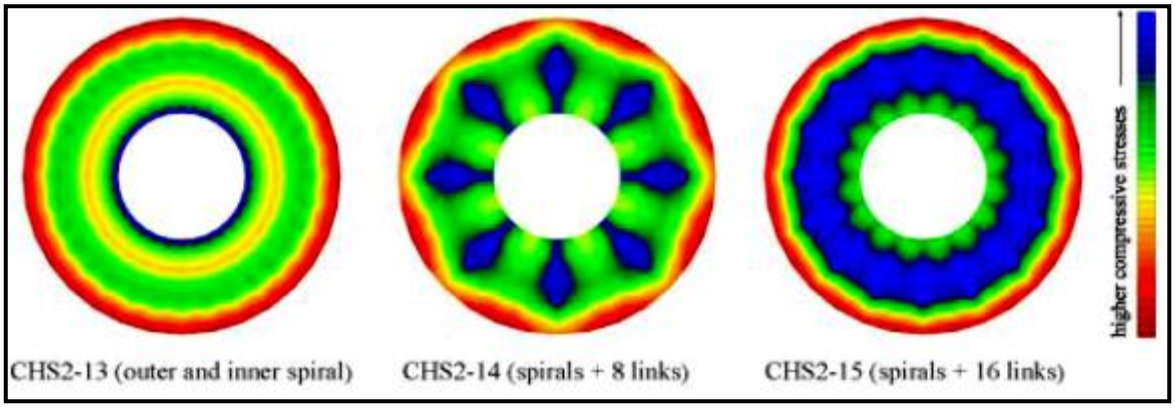


Figure 2.25 Contours of Axial Stress at Ultimate Strength for the CHS2 Circular Hollow Section without Transverse Links , with 8 Transverse Links and with 16 Transverse Links. (Papanikolaou et al , 2009)

In addition, the effect of negative confinement (cracking of the inner concrete cover) is diminished, because the confining action of the inner spiral is transferred by the links' tensile actions towards the outer spiral, providing improved confinement of the concrete region in-between.

## 2.5 EFFECT OF TYPE OF CONCRETE ON DUCTILITY OF PIERS.

**Xu et al. (2017)** perfomed experimental study on 14 test units to study seismic behavior of ultra-high-performance steel fiber reinforced concrete (UHPSFRC) columns. Based on a series of cyclic loading tests on specimens subjected to combined static axial loading and cyclic lateral loading, the investigation and analysis was done to understand the influence of stirrup spacing, type of stirrup, axial compression ratio and shear span ratio on the seismic performance of UHPSFRC columns.

The existence of steel fiber prevented the cracked concrete from spalling efficiently and delays the bulking of longitudinal reinforcement further as shown in Figure 2.26 below.

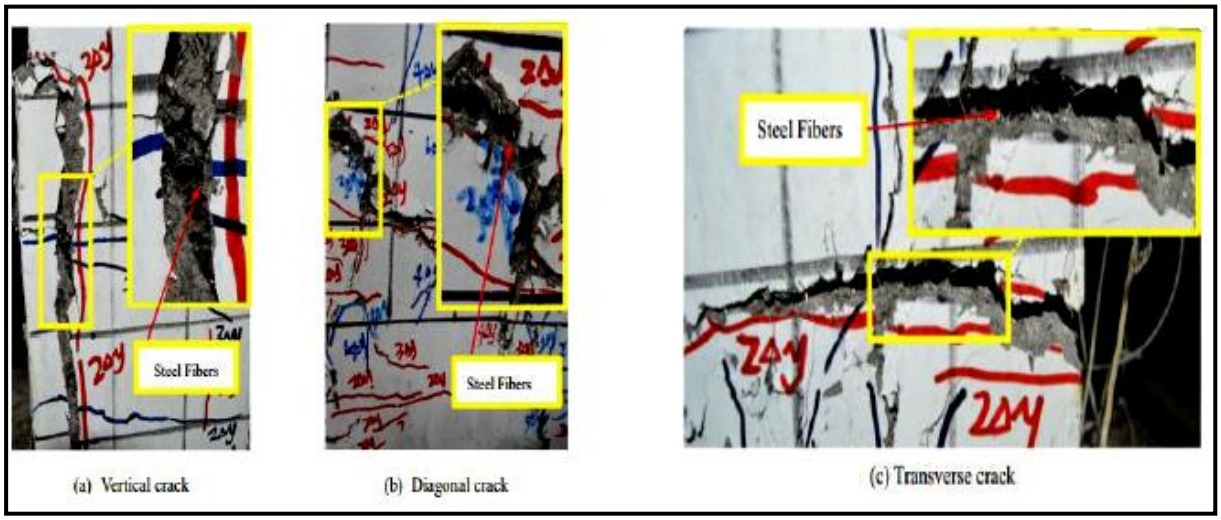


Figure 2.26 Steel Fiber Holding the Cracked Concrete ( Xu et al. 2017 )

Table 2.4 illustrates that a significant change of failure mode was made from a flexural-shear failure to a shear failure mode by increasing of the axial compression ratio since the higher axial compression could accelerate the slip between the shearing planes once the shear cracks appeared and restrain the development of horizontal cracks.

Table 2.4 Mode of Failure as per Shear Span/Depth ( Xu et al. 2017 )

| S.no | Shear span / Depth | Axial Load Ratio | Type of Failure |
|---|---|---|---|
| 1 | 5.3 | 0.20 | Flexural |
| 2 | 3.3 | 0.20 | Flexural-Shear |
| 3 | 3.3 | 0.36 | Shear |

The decreasing of stirrup spacing improved the deformation capacity, the ductility performance and the peak load in a certain range as the decreasing of stirrup spacing not only strengthened the shear resistant performance of specimens distributed to stirrups directly, but also improved the resistant performance of lateral force and deformation capacity indirectly by applying a more powerful confinement to the core UHPSFRC.

# CHAPTER 3
# METHODOLOGY

## 3.1 GENERAL

The main purpose of this dissertation was to take an industry-oriented research problem. One such problem encountered in the bridge design industry is the exact determination of length of zone of lateral confinement in slender bridge piers to ensure sufficient ductility. This length is a function of critical plastic region formed near the base of the pier and the study here aims to determine the zone of critical plastic region analytically. A Finite Element Analysis was performed using MIDAS FEA software package. A total of twenty-seven models were analyzed by the software to study the effect of percentage of longitudinal reinforcement, axial load ratio and amount of shear reinforcement on plasticity status and crack pattern keeping the grade of concrete and steel uniform .Nonlinear static analysis for each model was performed by defining a load set in which a uniform lateral deformation at the top was provided along with axial load acting simultaneously. Out of these twenty seven models, nine models were also subjected to five step incremental lateral loading at an axial load ratio of 8%.The geometric modeling and meshing details were kept same for each model but the longitudinal reinforcement details and shear reinforcement details were varied and the same have been described in the next section.

## 3.2 GEOMETRIC AND MODELLING DETAILS

The hypothetical slender pier was modeled as a solid in MIDAS FEA using primitive box element feature. The height of the box was kept as 7000 mm and the other two dimensions as 500 mm X 500 mm to maintain the slenderness ratio of 14 in both plan directions. A total of 27 models were analyzed reinforcement in longitudinal direction was modeled using 3-D line element. The clear cover for longitudinal reinforcements in all the models was kept as 40 mm.The total number of reinforcing bars and the spacing of the reinforcement in a particular model varies as per the percentage of reinforcement provided in a particular model. The lateral ties are modeled as rectangular curve on the work plane to simulate stirrups in actual pier. The spacing of lateral ties vary as per percentage by volume provided in each model**.** The figure below shows geometric details of the model.

The percentage of longitudinal reinforcement was varied as 1.5%, 2% and 3%.For each percentage of longitudinal reinforcement, the percentage of shear reinforcement was kept as 0.5%, 1% and 1.5.

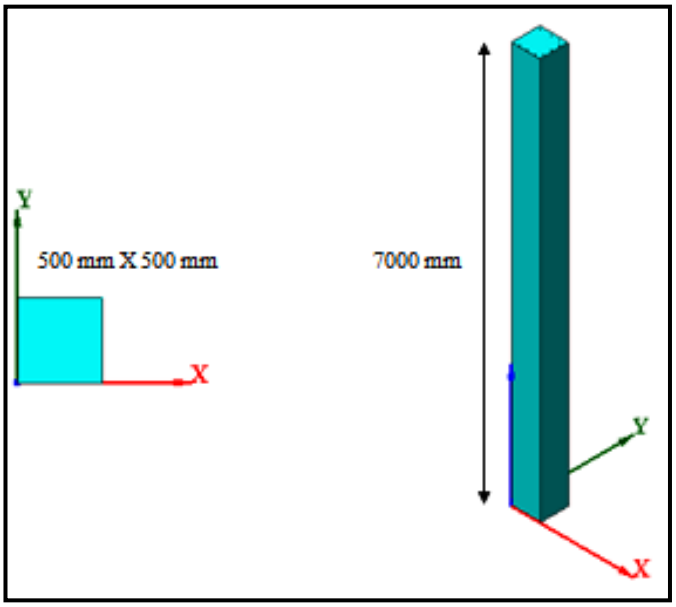


Figure 3.1 Geometric Details Common to all Models (MIDAS FEA)

Three axial load ratios were considered varying as 6%,7%,8% . Hence for each percent of axial load ratio, a total of 9 models were analyzed this way a total of 27 different models were analyzed using MIDAS FEA. Following figure shows the image of a particular model without meshing properties to get an insight about the modeling details.

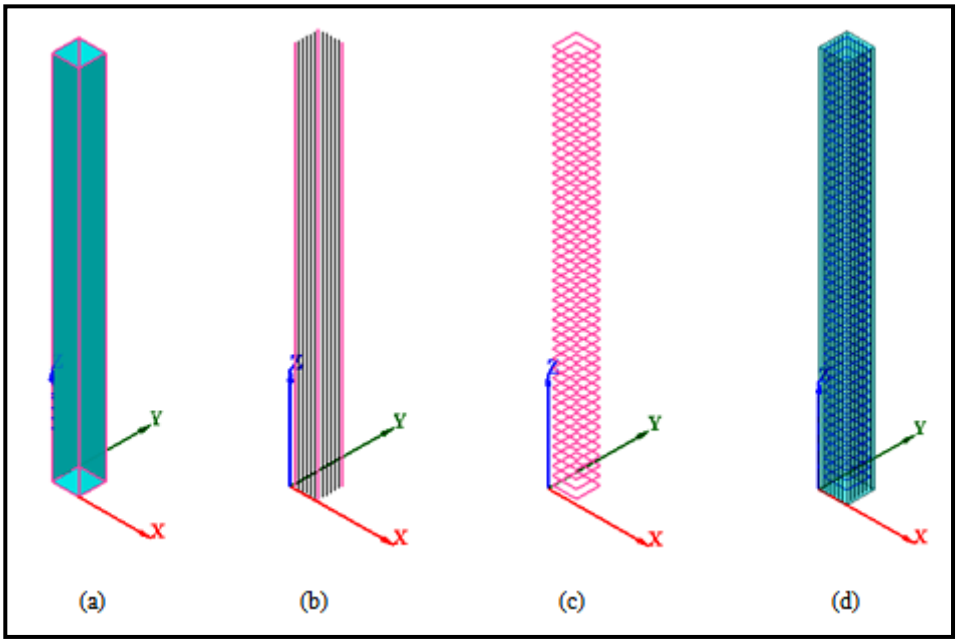


Figure 3.2 Elements Used for Modeling (MIDAS FEA)

In the above figure (a) is the solid primitive box element , (b) is the longitudinal reinforcement modeled as 3D line , (c) is the lateral ties modeled as rectangular curve (d) is the complete model including solid geometry along with longitudinal and lateral reinforcement.

In order to clearly differentiate the models, they were named in a specific manner based on the percentage of longitudinal reinforcement, percentage by volume of lateral ties present and axial

load ratio applied on the model. For example,1.5-0.5-6 refers to the model having 1.5 percent longitudinal reinforcement along with 0.5 percent by volume of lateral ties and subjected to axial load ratio of 6 percent. The details of all the models is shown in Table 3.1

Table 3.1 Details of all the Models Used in Present Study

| Model No | Name | Percentage of longitudinal reinforcement | Percentage by volume of shear reinforcement | Axial Load Ratio(%) | Spacing between Lateral ties (mm) |
|---|---|---|---|---|---|
| 1 | 1.5-0.5-6 | 1.5 | 0.5 | 6 | 152 |
| 2 | 1.5-1.0-6 | 1.5 | 1.0 | 6 | 076 |
| 3 | 1.5-1.5-6 | 1.5 | 1.5 | 6 | 051 |
| 4 | 2.0-0.5-6 | 2.0 | 0.5 | 6 | 152 |
| 5 | 2.0-1.0-6 | 2.0 | 1.0 | 6 | 076 |
| 6 | 2.0-1.5-6 | 2.0 | 1.5 | 6 | 051 |
| 7 | 3.0-0.5-6 | 3.0 | 0.5 | 6 | 152 |
| 8 | 3.0-1.0-6 | 3.0 | 1.0 | 6 | 076 |
| 9 | 3.0-1.5-6 | 3.0 | 1.5 | 6 | 051 |
| 10 | 1.5-0.5-7 | 1.5 | 0.5 | 7 | 152 |
| 11 | 1.5-1.0-7 | 1.5 | 1.0 | 7 | 076 |
| 12 | 1.5-1.5-7 | 1.5 | 1.5 | 7 | 051 |
| 13 | 2.0-0.5-7 | 2.0 | 0.5 | 7 | 152 |
| 14 | 2.0-1.0-7 | 2.0 | 1.0 | 7 | 076 |
| 15 | 2.0-1.5-7 | 2.0 | 1.5 | 7 | 051 |
| 16 | 3.0-0.5-7 | 3.0 | 0.5 | 7 | 152 |
| 17 | 3.0-1.0-7 | 3.0 | 1.0 | 7 | 076 |
| 18 | 3.0-1.5-7 | 3.0 | 1.5 | 7 | 051 |
| 19 | 1.5-0.5-8 | 1.5 | 0.5 | 8 | 152 |
| 20 | 1.5-1.0-8 | 1.5 | 1.0 | 8 | 076 |
| 21 | 1.5-1.5-8 | 1.5 | 1.5 | 8 | 051 |
| 22 | 2.0-0.5-8 | 2.0 | 0.5 | 8 | 152 |
| 23 | 2.0-1.0-8 | 2.0 | 1.0 | 8 | 076 |

| | | | | | |
|---|---|---|---|---|---|
| 24 | 2.0-1.5-8 | 2.0 | 1.5 | 8 | 051 |
| 25 | 3.0-0.5-8 | 3.0 | 0.5 | 8 | 152 |
| 26 | 3.0-1.0-8 | 3.0 | 1.0 | 8 | 076 |
| 27 | 3.0-1.5-8 | 3.0 | 1.5 | 8 | 051 |

For all the models , the material properties , diameter of longitudinal reinforcement , diameter of lateral ties was kept same. The following table shows the details of the factors common to all the models.

Table 3.2 Parameters Common to all the Models (MIDAS FEA)

| S No | Description | Value |
|---|---|---|
| 1 | Grade of concrete | M40 |
| 2 | Grade of longitudinal reinforcement | Fe 500 |
| 3 | Grade of shear reinforcement | Fe 415 |
| 4 | Diameter of longitudinal reinforcement | 20 mm |
| 5 | Diameter of shear reinforcement | 12 mm |
| 6 | Modulus of elasticity of concrete | 31622 $N/mm^2$ |
| 7 | Modulus of elasticity of steel | 205000 $N/mm^2$ |
| 8 | Poisson's Ratio for concrete | 0.2 |
| 9 | Poisson's ratio for steel | 0.3 |

## 3.3 CONSTITUTIVE MODELS AND FUNCTIONS

To study the crack pattern and plasticity status of the slender pier models , some constitutive models were adopted .MIDAS FEA supports a large variety of constitutive models , with the liberty of user defined model as well. In the present study , the models used for concrete and steel are shown in Table 3.3 and some basic details regarding the same are described in the upcoming paragraphs.

### 3.3.1 Total Strain Crack Model

Various discrete and smeared concrete crack models are available in the literature which have further classifications as well. In our study total strain crack model for defining crack status of

concrete was considered which falls in the category of smeared crack model. . The basic reason of selecting total strain crack model over other smeared crack models (e.g. the decomposed strain model) was its easy algorithm since this model needs only one stress strain relationship to predict tensile behavior that include cracks and another relationship to determine the compressive behavior.

Also, we were only interested in the determination of total strain rather than individual strains contributing to total strain e.g. elastic strain ,creep strain, thermal strain,etc.Another advantage of selecting the total strain crack model was its more practical behavior as the input data regarding material properties required for the study of nonlinear behavior is relatively simple and the convergence is fast.

The figure below shows the two widely accepted further classifications of total strain crack model based on reference crack axis.In Figure (a) depicts the fixed axis model while (b) depicts the rotating crack model.

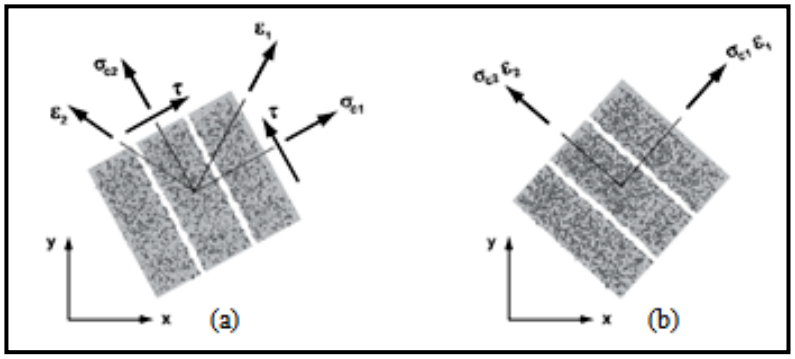


Figure 3.3 Fixed Axis Model and Rotating Crack Model (MIDAS FEA Manual)

Table 3.3 Constitutive Models Used in the Study.

| S No | Material | Model Name | Type |
|---|---|---|---|
| 1 | Concrete | Total Strain Crack | Isotropic |
| 2 | Longitudinal Reinforcement | Von Mises | Isotropic |
| 3 | Shear Reinforcement | Von Mises | Isotropic |

In Figure 3.3 it can be seen that only normal stress is present in the rotating crack model while both shear stress and normal stress is shown in the fixed crack model.The main reason behind this is the fact that in the fixed crack model the direction of the new cracks remain unchanged thus both stresses exist on the crack surface.This is not true for the rotating crack model as new cracks in the rotating crack model develop in the direction of current principle strain and hence

the cracks developed at the previous stage are ignored.

Prior to cracking the concrete material exhibits isotropic properties which turn into anisotropic after cracking.However MIDAS considers orthotropic properties as soon as the concrete is cracked.Also MIDAS uses Modified Compression Theory proposed by Selby and Vecchio for the constitutive model based on total strain .

*3.3.1.1 Tension Models in Total Strain Crack*

The tensile behavior of concrete is controlled by the formation of micro cracks and if the tensile stress reaches a certain limit (e.g. 3 N/mm$^2$), the additional deformation gets localised within the region and this is known as a fracture process zone.After the tensile limit is reached the stress in those regions decreases as the strain increases.When the tensile stress approaches zero a macro crack is formed in the fracture zone. This phenomenon is called as tension softening.There are various models that simulate such a process. Out of various models available in MIDAS FEA Hordjik Model is selected for analysis.Some brief description of the model is given below.

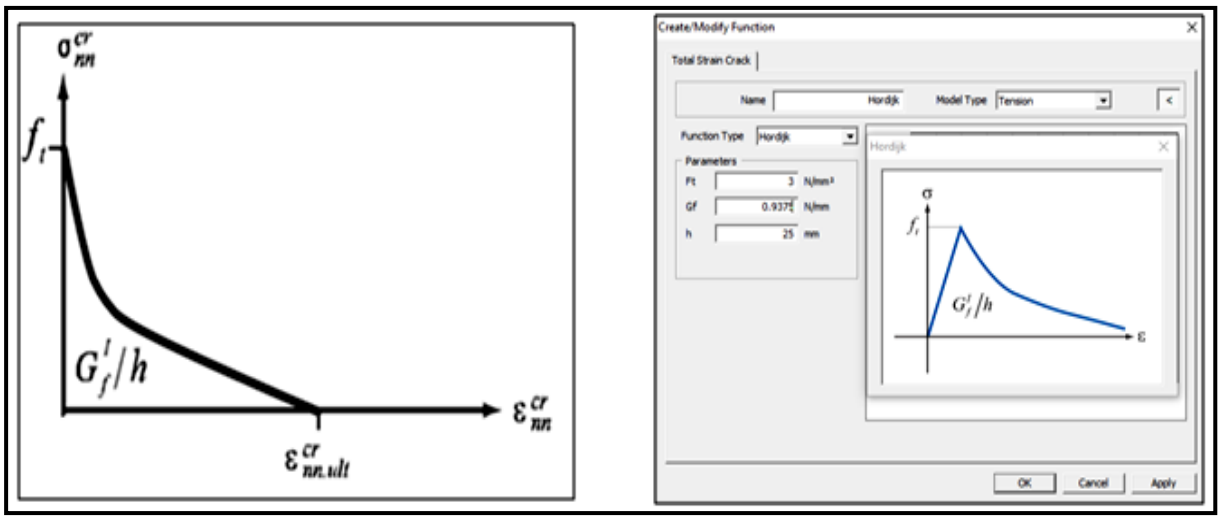


Figure 3.4 Hordjik Model Used as Tension Model (MIDAS FEA)

MIDAS FEA gives the option to the user to input the above values that can be used to predict tension softening behavior of the concrete. The same is shown in Figure 3.4 .Following equation is used to calculate tensile fracture energy.

$$f_t = \left(0.739 \frac{G_f^I E}{h}\right)^{1/2} \quad (7)$$

Table 3.4 Parameters to Define Hordjik Model

| S.No | Description | Symbol | Value used in analysis |
|---|---|---|---|
| 1 | Tensile Strength | $f_t$ | 3 N/mm$^2$ |
| 2 | Tensile fracture energy | $G^I_f$ | 0.009735 N/mm |
| 3 | Crack band width | $h$ | 25 mm |

*3.3.1.2 Compression Models in Total Strain Crack*

MIDAS FEA includes six different type of compression models e,g. elastic model , ideal model, Thorenfeldt model, linear hardening model , multi-linear hardening model, saturation model and parabolic model .In the present study Thorenfeldt model was adopted which has the following curve associated with it.

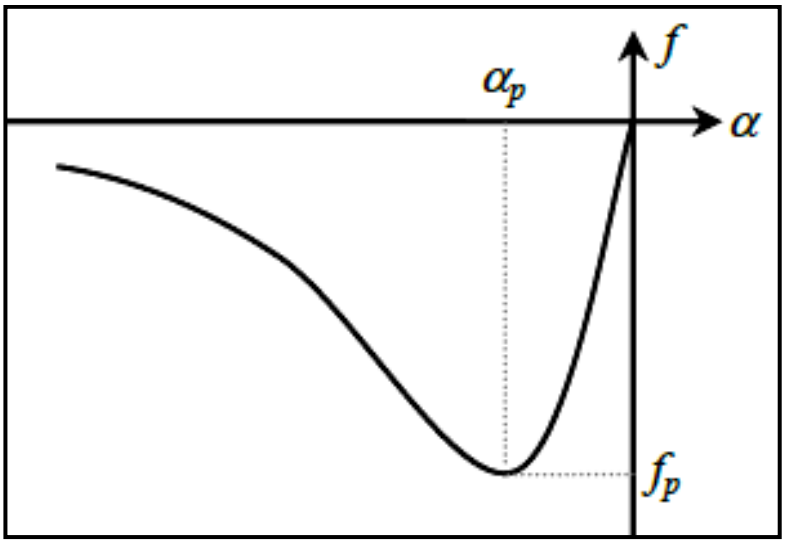


Figure 3.5 Thorenfeldt Model Curve (MIDAS FEA Manual)

For the compression models in tension strain crack , the compressive behavior was assumed to be linearly elastic up to 30 % of uniaxial strength, $f_c$.i.e. up to 30 percent it will behave as elastic and beyond that limit non-linearity is observed.

*3.3.1.3 Other functions for defining Total Strain Crack*

Apart from the compression and tension models discussed in the previous section , there are other functions also which influence the total strain crack model.Table 3.5 below shows the functions that are being considered in the present study for proper execution of total strain crack model.

Table 3.5 Functions Used for Defining Total Strain Crack Analysis (MIDAS FEA)

| S No | Function Name | Model available in MIDAS FEA | Model adopted for analysis |
|---|---|---|---|
| 1 | Crack Model | (i) Fixed , (ii) Rotating | Fixed |
| 2 | Stiffness Matrix | (i) Tangent , (ii) Secant | Secant |
| 3 | Lateral Crack Effect | (i) Vecchio and Collins | Vecchio and Collins |
| 4 | Confinement Effect | (i) Selby and Vecchio | Selby and Vecchio |
| 5 | Shear Function | (i) Elastic , (ii) Constant (iii) Multilinear | Elastic |

Because of the non-linearity involved in the concrete crack analysis an iterative scheme is used. These incremental iterative procedures require the constitutive model to be defined by a proper stiffness matrix. In MIDAS FEA , two approaches are available for defining the stiffness matrix. The tangent stiffness matrix approach is considered more suitable for studies where pattern of crack propagation is of prime interest. However, the secant stiffness matrix approach is more appropriate for studies involving reinforced concrete structures where cracks are developed widely. In the present study the secant approach is used with zero Poisson's ratio in all directions considering the stiffness of an orthotropic material which gives a matrix in the principal coordinate system.

When the concrete is in tension and it is subjected to compression parallel to the crack direction, the compressive strength and stiffness will be reduced as per Lateral Crack Model by Vecchio and Collins. If the concrete is subjected to biaxial or compressive stresses , the compressive strength increases due to the effect of confinement. This confinement effect is taken into account using Selby and Vecchio model in the cracked concrete. If the tensile strains are perpendicular to the compressive direction, the compressive strength is reduced. This phenomenon of reduction in the compressive strength due to the tensile strains is called compression softening.

### 3.3.2 Von Mises Model

Both the shear and the longitudinal reinforcement were modeled as per Von Mises model without considering hardening of steel.This model is mostly used to analyse the metallic materials.It is based on determination of octahedral shear stress and yielding is assumed to occur when this regular octahedral shear stress reaches the limit defined by following equation.

$$f(\tau_{oct}) = (\tau_{oct}) \sqrt{\frac{2}{3}k} = 0 \quad (8)$$

## 3.4 MESH GENERATION

MIDAS FEA provides three types of mesh generation techniques i.e Aut o-Mesh , Mapped Mesh and Protrude Mesh. For a complex geometry, Auto-Mesh function is used which may include tetrahedron and triangular elements. However, before meshing the model , material property needs to be defined. For defining property of reinforcement, a separate 'Bar Section' is created that tells the program to treat the reinforcement as embedded reinforcement. If the reinforcement property is created without defining 'Bar Section' , then it is considered as non-embedded reinforcement.

### 3.4.1 Meshing of Solid Pier

In the current study the solid pier model was meshed using Map Mesh feature of MIDAS FEA.In this software the user has a choice of adjusting the mesh size of solid. Meshing of solid can either be done by selecting size of an element or by directly entering desired number of divisions of the solid geometry. Here the former method was applied, and the size of individual element was kept as 25 mm which was also the value of crack band width defined in table in previous section. It is preferred to use quadrilateral elements instead of triangular elements for simple geometry and to obtain more accurate results. Under the advanced tab in the Map Mesh feature , there is a choice of generating mid side nodes too , but in our study, we have not used the mid side node elements to obtain fast convergence. Figure 3.6 shows the meshing characteristics of solid pier model.

### 3.4.2 Meshing of Reinforcing Bars

The longitudinal reinforcement and the shear reinforcement in all the 27 models is meshed by using 'Edge method' under Auto-Mesh feature in MIDAS FEA.In the seeding method , we can choose various options available. In this study the seeding method adopted is based on number of divisions. Any desired number of divisions can be adopted as the reinforcement property defined prior to meshing is embedded type which maintains the compatibility with the solid pier even if there is no nodal connectivity.

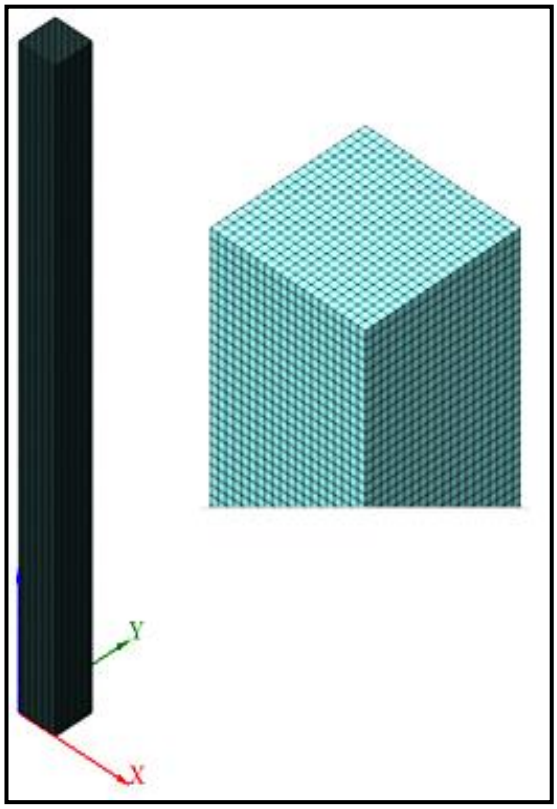


Figure 3.6 Meshing Details of Pier Model (MIDAS FEA)

Here the number of divisions adopted is 25.In the dialogue box, we have to select corresponding property e.g. property for shear rebars or longitudinal rebars depending upon whether shear reinforcement is being meshed or longitudinal reinforcement is being meshed. 'Bar in solid' is checked before meshing embedded reinforcement.

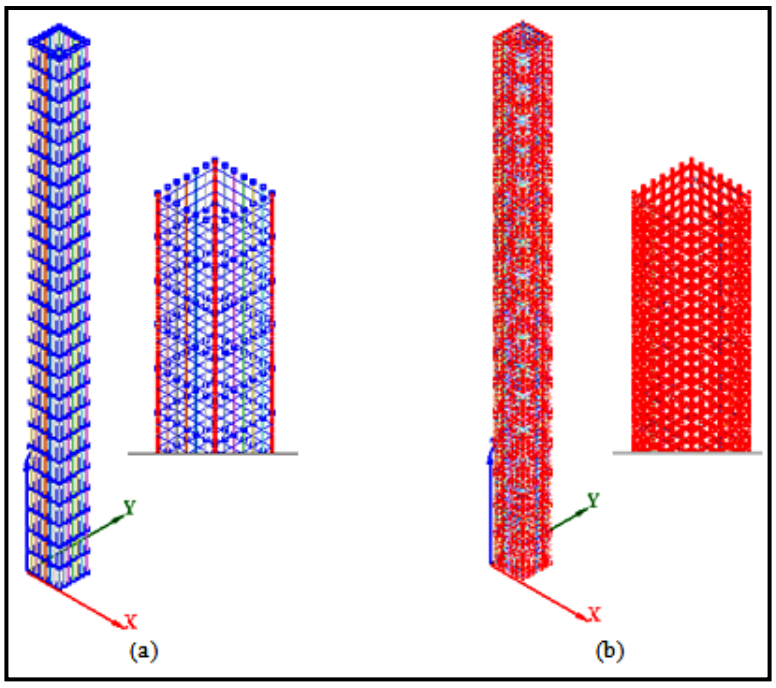


Figure 3.7 Meshing Details of Reinforcement (MIDAS FEA)

Table 3.6 Meshing Adopted for Finite Element Analysis (MIDAS FEA)

| S No | Description | Details |
|---|---|---|
| 1 | Size of single element | 25 mm x 25 mm x 25 mm |
| 2 | Total number of elements in each model | 112000 |
| 3 | Meshing technique for solid model | Map Mesh for solid |
| 4 | Meshing technique for reinforcement | Auto mesh along edge |
| 5 | Reinforcement type | Embedded |

## 3.5 LOAD AND BOUNDARY CONDITIONS

For certain cases where crack propagation or crack control analysis is to be studied the displacement-controlled loading is more convenient and reliable as the results obtained by this approach are more detailed and realistic in comparison to load controlled approach. This is due to the fact that the latter would not simulate the cracks quite well as the model may not converge or the analysis may end after the tensile stress has been exceeded.

### 3.5.1 Loading Scheme

In the current study a single load set was created in which the axial load ratio was applied as pressure load on the top along with a displacement induced loading applied at the top most nodes in the Y-Y direction. While the pressure load acting in the Z-Z direction varied as per the three axial load ratios considered, the lateral displacement applied at the top most nodes was taken 25 mm for all the 27 models. A rigid link was created to apply the displacement at top most nodes. The following table shows the axial load ratio and corresponding pressure load applied along global Z-Z direction on the top of the model along with the displacement applied at the top in the lateral direction. The following table shows the loading imposed on all the slender pier models analysed one at a time in MIDAS FEA.

Table 3.7 Loading Applied in Lateral and Axial Direction

| S.No | Axial load ratio (%) | Corresponding axial Pressure | Lateral Displacement |
|---|---|---|---|
| 1 | 6 | 2.4 $N/mm^2$ | 25 mm |
| 2 | 7 | 2.8 $N/mm^2$ | 25 mm |
| 3 | 8 | 3.2 $N/mm^2$ | 25 mm |

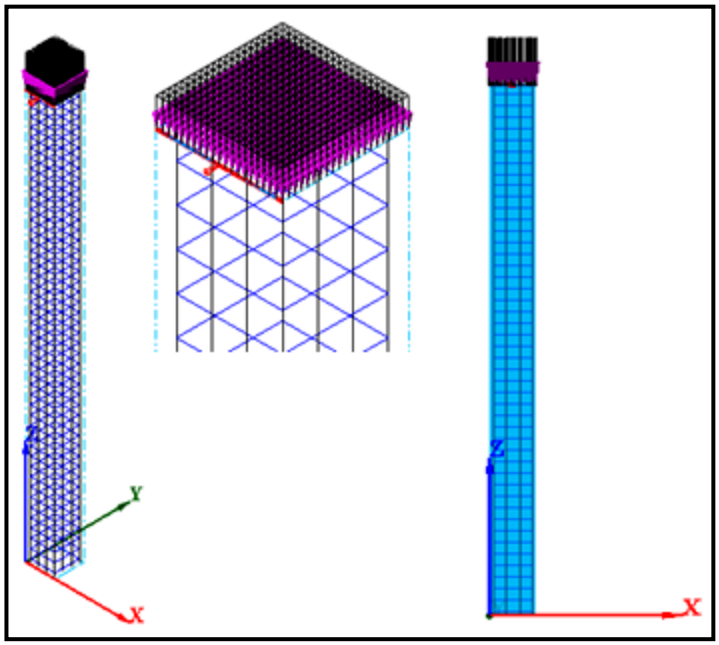


Figure 3.8 Details of Load Application (MIDAS FEA)

### 3.5.2 Boundary Conditions

All the nodes  at the bottom of the model were subjected to fixed boundary conditions with all deformations arrested and full constraint to all degrees of freedom.The fixed support conditions were adopted to simulate more realistic effect as the pier would be properly anchored inside the footing with almost full restraint on all degrees of freedom.The figure below indicates the boundary and loading conditions applied on a particular model.In total 441 nodes at the bottom were applied with fixed boundary conditions as shown in the figure below.

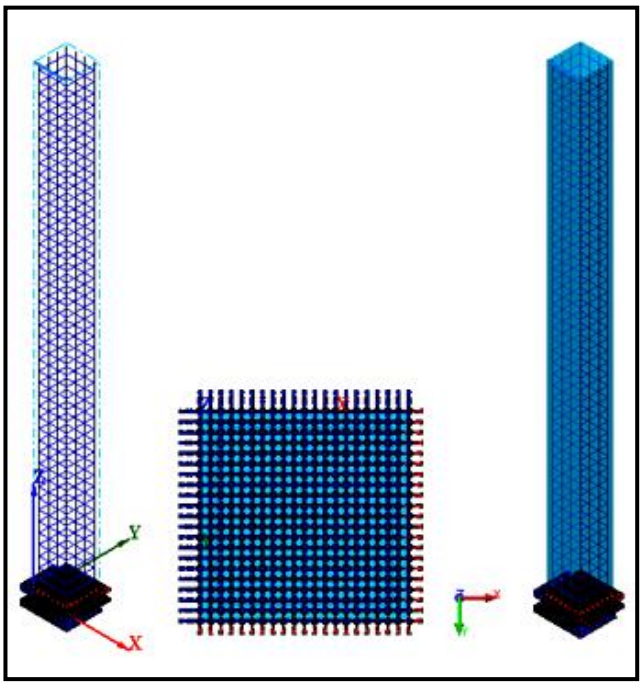


Figure 3.9 Boundary Conditions Applied to Nodes at the Base (MIDAS FEA)

## 3.6 ANALYSIS CASE AND ITERATION METHOD

The method and type of analysis to be used depends upon the main objective and purpose of the study.In the present study the main objective was to determine the zone of plasticity in a slender bridge pier.Plasticity usually involves a non linear material behavior and the analysis case was accordingly selected keeping in view the shift of material properties from elastic to plastic state.

### 3.6.1 Non-Linear Static Analysis

A non linear static analysis was adopted in the present study to understand the crack and plasticity status of different pier models with a common slenderness ratio of 14.The constitutive models as already described in previous section, were selected so as to define this particular type of analysis more realisticaly.While defining the analysis case, certain parameters like the type of output and points at which output is required (i.e element center or nodes) is also selected.In the present study the required analysis outputs that were selected are shown in the figure below.

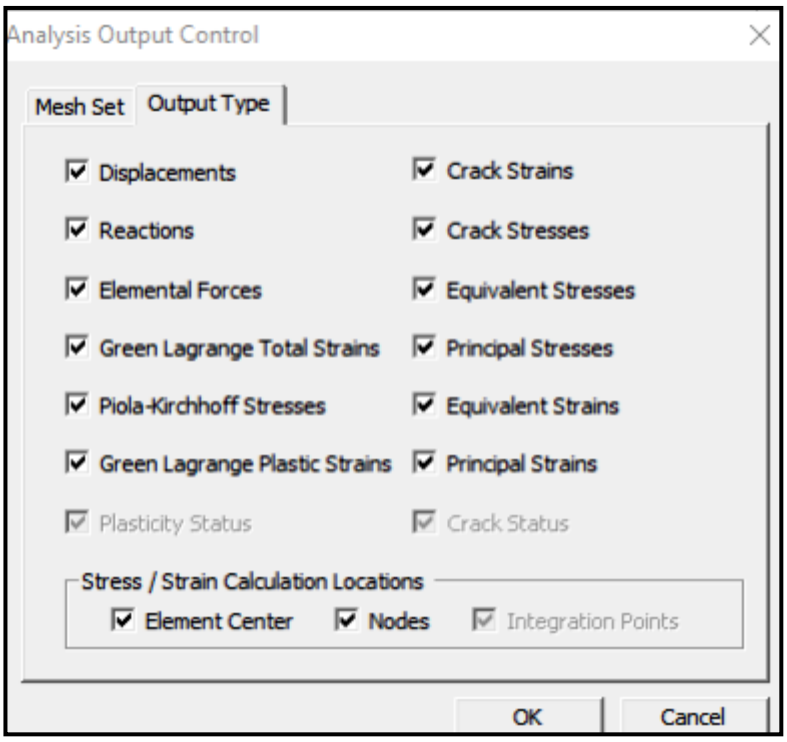


Figure 3.10 Outputs Available after Analysis (MIDAS FEA)

All the 27 models were subjected to the total lateral displacement of 25 mm applied without any load step increments simultaneously with axial pressure load that varied as per the axial load ratios.However in some of the models the total lateral displacement ( in Y-Y direction) was applied in five step increments also for more detailed analysis.

### 3.6.2 Iteration Method

In performing non linear finite element analysis , it is required to determine a displacement vector that would equate the internal and external forces to maintain equilibrium.For this purpose the problem has to made discrete both in space i.e. with finite elements and in time i.e with increments.In order to fulfill equilibrium requirement at the end of each increment, an iterative procedure is adopted.

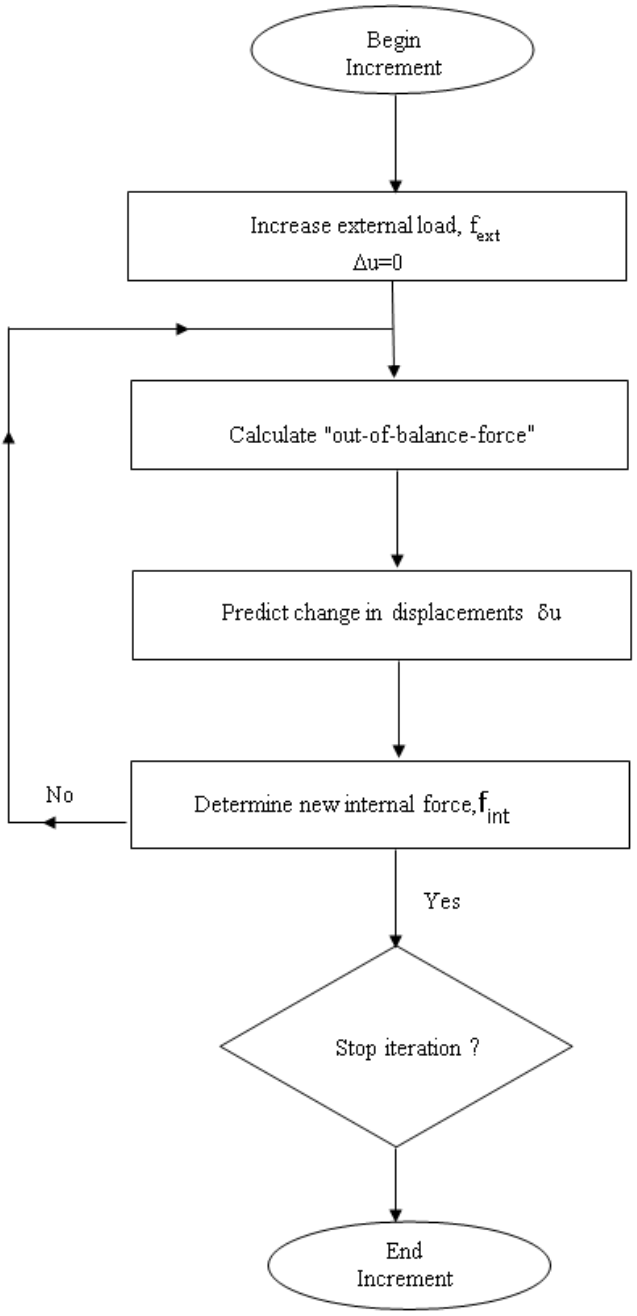


Figure 3.11 Iteration Process (MIDAS FEA Manual)

In the present study Newton Raphson method was used as the method of iteration with maximum number of iterations per increment kept as 200.

As mentioned earlier, apart from directly applying displacement induced loading in Y-Y direction in a single increment, some models were also subjected to 25 mm lateral displacement in five step increments for detailed and accurate analysis.If a certain increment fails to converge even after undergoing 200 interations , then the analysis was terminated automatically by the MIDAS solver.

*3.6.2.1 Convergence Criteria*

Every iteration process is expected to converge as soon as the conditions defined for convergence are met and the results are satisfactory. Once the convergence is obtained all the iterative processes are stopped. The iteration process is also stopped if a certain specified maximum number of iterations has been reached which actually indicates that the solution is diverging.

The convergence criteria are based on certain norms and in MIDAS FEA there are three norms available on the basis of which the criteria for convergence are defined. These are mentioned in the following table and the one adopted in current study is also shown in the last column.

Table 3.8 Convergence Criteria

| S No | Convergence Criteria in MIDAS FEA | Criteria Adopted |
|---|---|---|
| 1 | Energy Norm | Energy Norm |
| 2 | Force Norm | |
| 3 | Displacement Norm | |

The energy norm adopted here is composed of internal forces (and not the unbalanced force) along with the relative displacements.Energy ratio is calculated to determine the level of convergence.

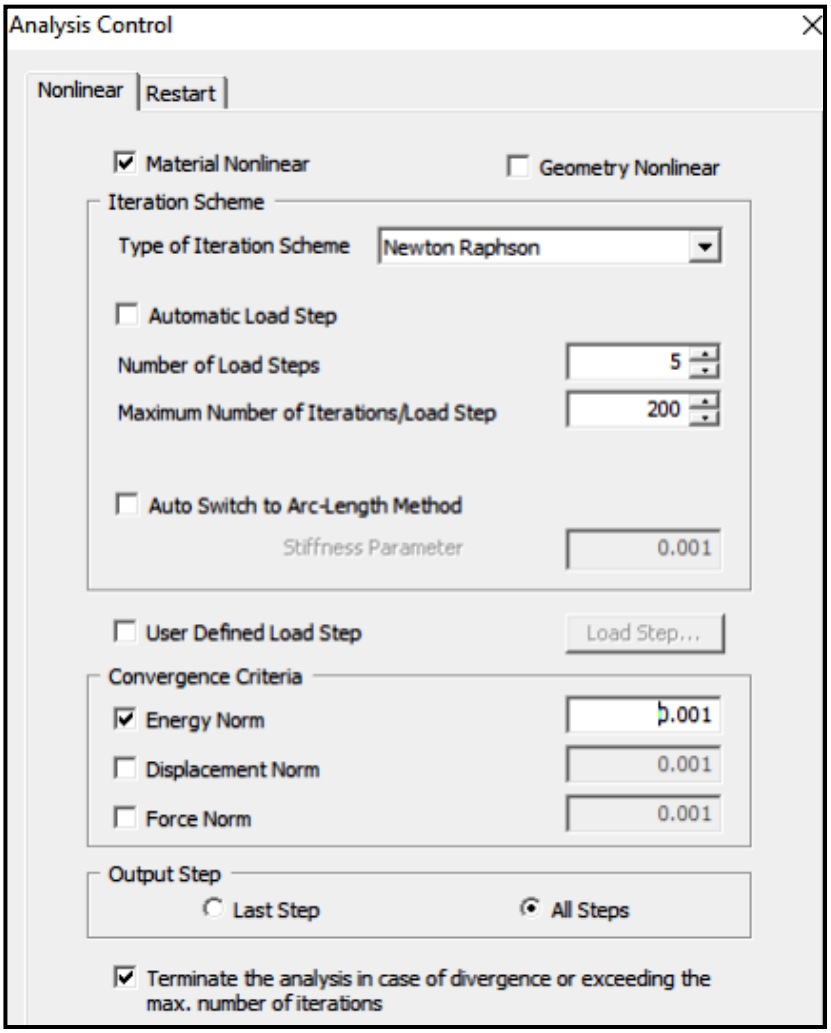


Figure 3.12 Iteration Scheme and Convergence Criteria Adopted (MIDAS FEA)

# CHAPTER 4
# RESULTS AND DISCUSSION

## 4.1 GENERAL

The results obtained after analyzing all the 27 models were sorted and grouped in such a way so that the effect of variation of all the three factors considered in the present work could be studied effectively. Out of all the results obtained, only the results corresponding to the plasticity status and the fully cracked (open) zone have been described in this chapter. Relevant images obtained from the software analysis are also presented to clearly describe the plasticity status and fully cracked zone of all the models for a more realistic understanding of the study. Graphical representation of the corresponding results is also presented in which one factor is kept constant and the effect of variation of other two factors on the plasticity and crack zone has been studied. Based on the observations made, the possible reasons for the variation in zone of plasticity and cracks with the change in factors considered have been discussed. Nine models were subjected to incremental loading also and the results obtained for these models have been presented in the last section of this chapter.

## 4.2 RESULTS FOR CONSTANT AXIAL LOAD RATIO

In this section the results are presented considering constant axial load ratio. For three different axial load ratios (i.e. 6% , 7% , 8%), results are presented in three different sub-sections. Nine models per axial load ratio were grouped together based on the longitudinal and lateral reinforcement provided. In each section , first the images obtained after analysis are shown and then the results are presented as graphical representation as per the variation of other two factors i.e. percentage of longitudinal reinforcement and amount of lateral ties expressed as percent by volume.

In the images obtained from analysis, the blue color zone depicts the zone of plasticity while the red color zone represents fully open or total cracked zone. The grey color depicts the portion of the model that is uncracked and still elastic.

### 4.2.1 Axial Load Ratio : 6 %

The plasticity status of the meshed elements and fully cracked zone of nine models subjected to axial load ratio of 6 % , ( i.e. 2.4 $N/mm^2$ pressure applied on top of the pier) is presented in Figure 4.1.These results were extracted individually for each model and compiled and placed adjacent to each other to facilitate effective comparison. It can be clearly seen from Figure 4.1 and Figure 4.2 that the length of the zone where fully open cracks are spread (marked red) is

increasing as the percentage of lateral ties decreases for a particular percentage of longitudinal reinforcement.

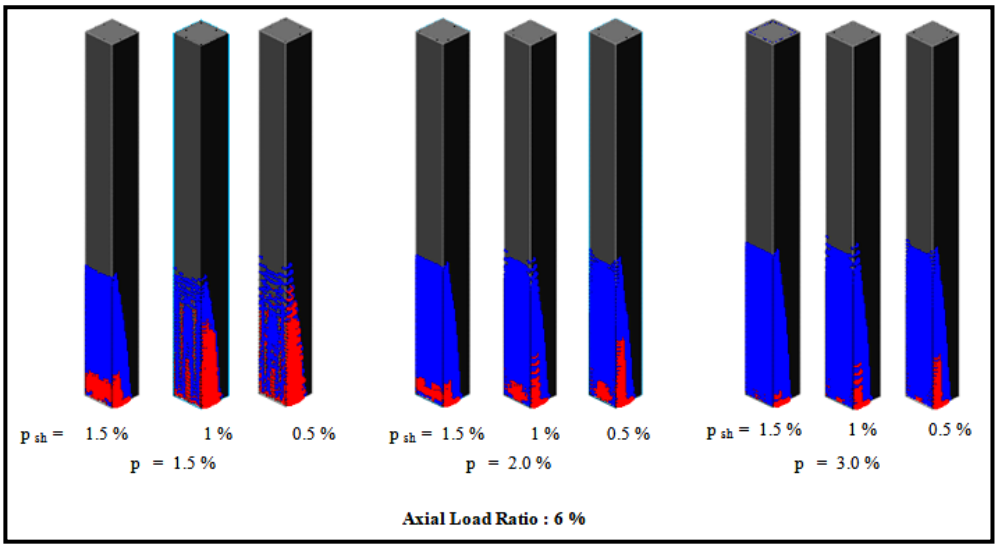


Figure 4.1 Height of Fully Open Cracked Zone for Axial Load Ratio : 6% (MIDAS FEA)

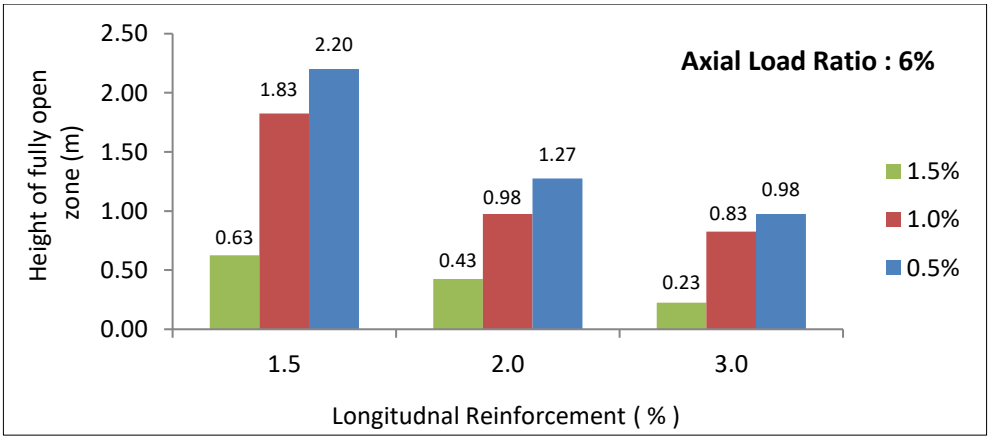


Figure 4.2 Graphical Representation of Results for Axial Load Ratio: 6%

This is because with the decrease in volumetric percentage of lateral reinforcement the spacing between the individual ties increases. Here the variation in spacing is 51 mm, 76 mm and 152 mm for percentage of lateral reinforcement 1.5, 1.0 and 0.5 respectively. For a lesser spacing the chances of cracked concrete to spall away is less in comparison to the models with larger tie spacing. The part of concrete which may exceed tensile stresses more than the rupture stress is effectively confined for a lesser tie spacing, although the stresses in ties may increase. These results indicate that as the percentage of lateral reinforcement is increased the height of fully open cracked zone decreases. However, this does not mean that we should increase the percentage of lateral reinforcement as 2% or 2.5% to further decrease this height of fully open cracked concrete. This is because the clear spacing between the ties should never be lesser than

the maximum size of aggregate used in concrete to allow concrete to be effectively poured and moved at the time of casting. If the lateral reinforcement is increased beyond a certain percentage, there are chances that the steel ties may not be properly embedded on all sides in the surrounding concrete and the composite action between steel and concrete may not be effective.

Figure 4.2 is the graphical representation of data obtained from Figure 4.1. It clearly indicates that with the increase in percentage of longitudinal reinforcement from 1.5 to 3 ,the height of fully open cracked zone decreases for all percentages of lateral ties. With the increase in percentage of longitudinal reinforcement , the number of reinforcing bars present at a particular face increases ( since diameter of the bar is kept constant in the present study).This means for same amount of stresses , more bars are available to share the stress and also the concrete is more confined for a particular spacing of lateral ties , since on increasing the number of longitudinal bars for a particular lateral reinforcement, the spacing between longitudinal bars decreases which means a decrease in the area available for the cracked concrete to spall away. Another important observation made from Figure 4.1 is that although the height of cracked zone for higher amount of lateral reinforcement (corresponding to particular longitudinal reinforcement ) is less but the spread of cracked zone along the width ( X-X direction) is more.

4.2.1 Axial Load Ratio : 7 %

For constant axial load ratio of 7% (i.e. axial pressure of 2.8 $N/mm^2$) the results obtained from the software output window are shown in Figure 4.3 for different reinforcement arrangements. The observations in this case are similar to the observations made for axial load ratio of 6%.As the percentage of longitudinal reinforcement is increased, the spread of fully open cracked zone is reduced for each percentage of lateral reinforcement. The reasons for such a behavior are already discussed in the previous section.

From Figure 4.3 it can be observed that the spread of fully cracked zone in the X-X direction along the width of the models is more for lower longitudinal reinforcement having higher percentage of lateral ties. This spread along the width decreases as the percentage of longitudinal reinforcement is increased for all percentages of lateral reinforcement.

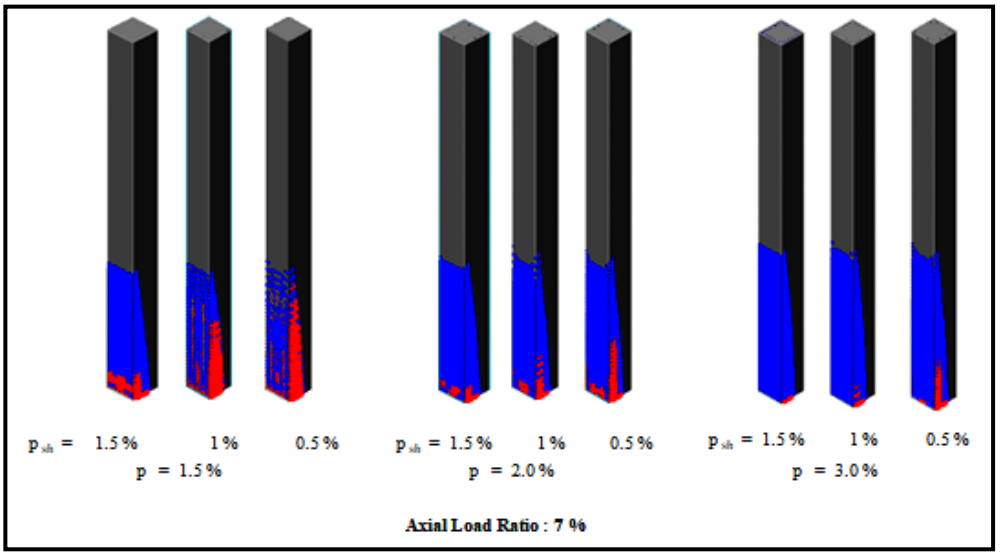


Figure 4.3 Height of Fully Open Cracked Zone for Axial Load Ratio : 7% (MIDAS FEA)

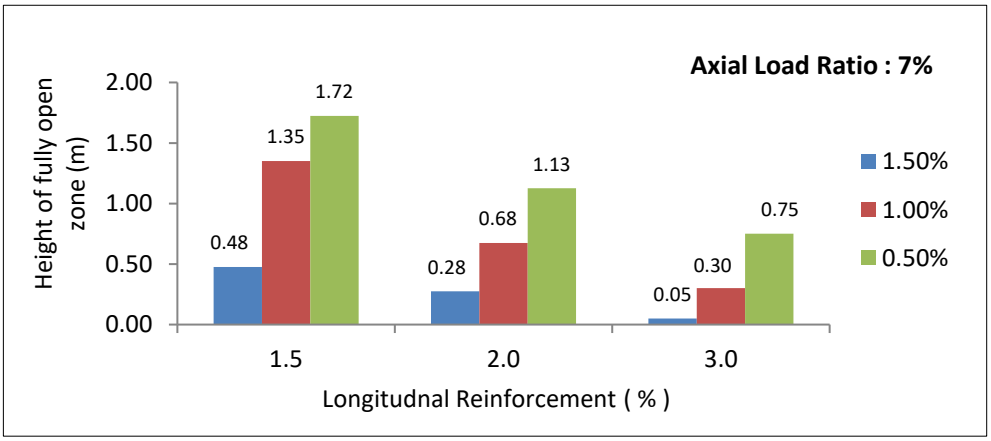


Figure 4.4 Graphical Representation of Results for Axial Load Ratio : 7%

### 4.2.3 Axial Load Ratio : 8 %

For axial load ratio of 8% , similar trend was observed as for other two axial load ratios, regarding the zone of fully cracked portion of the models with different reinforcement arrangements.

The increase in longitudinal reinforcement percentage along with the increase in percentage of lateral ties resulted in a reduced height of fully open cracked zone as shown in Figure 4.5.Also for model with 3% longitudinal reinforcement , almost zero length of fully open cracked zone along the width ( X-X direction) was observed as indicated in the figure below.

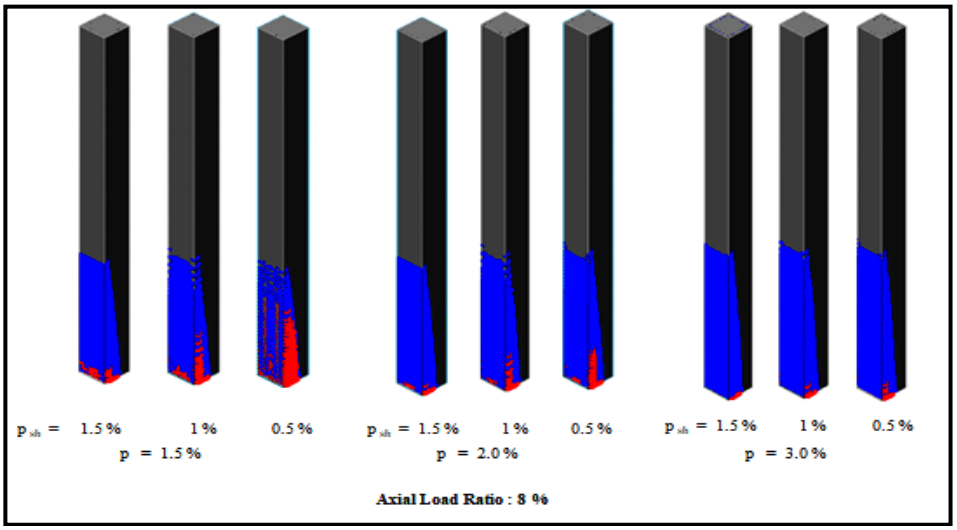


Figure 4.5 Height of Fully Open Cracked Zone for Axial Load Ratio : 8% (MIDAS FEA)

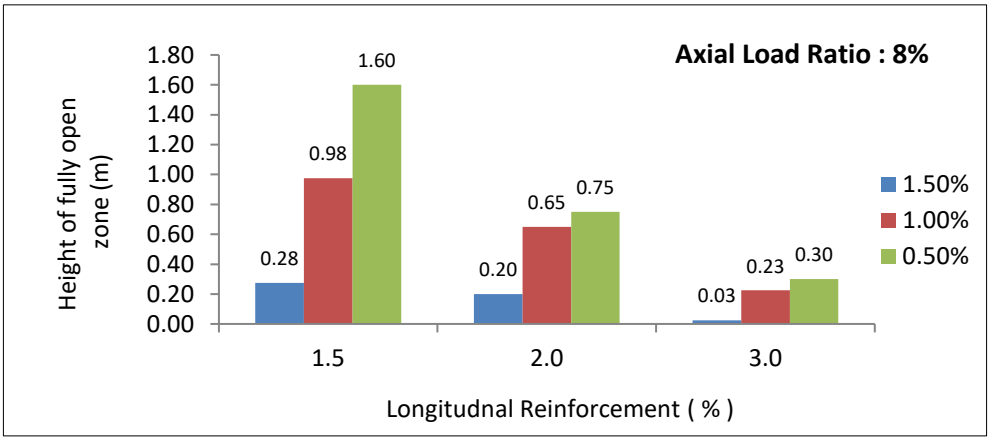


Figure 4.6 Graphical Representation of Results for Axial Load Ratio : 8%

From the above graph it can be seen that for axial load ratio of 8% , almost no fully open zone was obtained for model with 3% longitudinal reinforcement and 1.5% lateral reinforcement. This is reasonable as a heavily reinforced section will leave less space for the concrete that may be cracked to bulge or fall out and, in this case, although it may be cracked but still be in place and fully open voids due to concrete spalling out is avoided.

The percentage decrease of fully open cracked height was calculated using the above results and has been tabulated below for all the values of different factors considered in the present study. The table indicates that as the axial load ratio is increased from 6% to 8% , the fully open crack height decreases by following percentages for different combinations of lateral and longitudinal reinforcement. It can be seen that maximum percentage of decrease occurs for the pier model with maximum lateral reinforcement(i.e. 1.5%) and maximum longitudinal reinforcement (i.e. 3.0 %) when axial load changes from 6% to 8%.Also the minimum variation in fully cracked height corresponds to the model with least lateral and longitudinal

reinforcement when axial load ratio was varied from 6 % to 8 %.

Table 4.1 Percentage Decrease in Height of Fully Open Zone due to Increase in Axial Load Ratio From 6% to 8%

| **Percentage of Lateral Reinforcement** | **Percentage of longitudinal reinforcement** | | |
|---|---|---|---|
| | **3.00 %** | **2.00 %** | **1.50 %** |
| **0.5 %** | 69.4 % | 41.4 % | 27.2 % |
| **1.0 %** | 72.3 % | 33.7 % | 46.4 % |
| **1.5 %** | 87.0 % | 53.5 % | 55.5 % |

## 4.3 RESULTS FOR CONSTANT LATERAL REINFORCEMENT

The height of fully open zone from the base of the pier model subjected to lateral displacement and an axial load simultaneously, is presented in the following three graphs in which the volume of lateral reinforcement is kept uniform for varying percentage of longitudinal reinforcements and different axial load ratios.It was observed that for a particular amount of lateral reinforcement , the height of fully open cracked zone increases as the percentage of longitudinal reinforcement decreases. It has already been discussed in the previous sections that with the increase in amount of reinforcement there is a reduction in the area from where concrete when cracked can spall off when subjected to compressive and bending loads.

Almost negligible change in the height of fully open zone was observed for models having axial load ratios 7% and 8% (being 0.68 m to 0.65 m only) with 2% of longitudinal reinforcement at 1% lateral reinforcement. However significant variation in the reduction of this cracked height was observed for other axial load ratios at a particular longitudinal steel and uniform amount of lateral reinforcement. The same can be referred from Figure 4.7.

From Figure 4.8 and Figure 4.9 it can be observed that very slight decrease in the height of fully open cracked zone is seen when axial load ratio increases from 6% to 7% for the model with highest percentage of longitudinal reinforcement .

From Table 4.2 it can be seen that the decrease in height of fully open crack zone due to increase in percentage of lateral reinforcement from 0.5 % to 1.5 % is maximum (being more than 90%) for the model having maximum longitudinal reinforcement of 3% and subjected to higher axial loads. Also from the table it can be concluded that on an average 78 % decrease in height of fully open cracked zone was observed as the percentage of lateral reinforcement was increased from 0.5 % to 1.5 %.

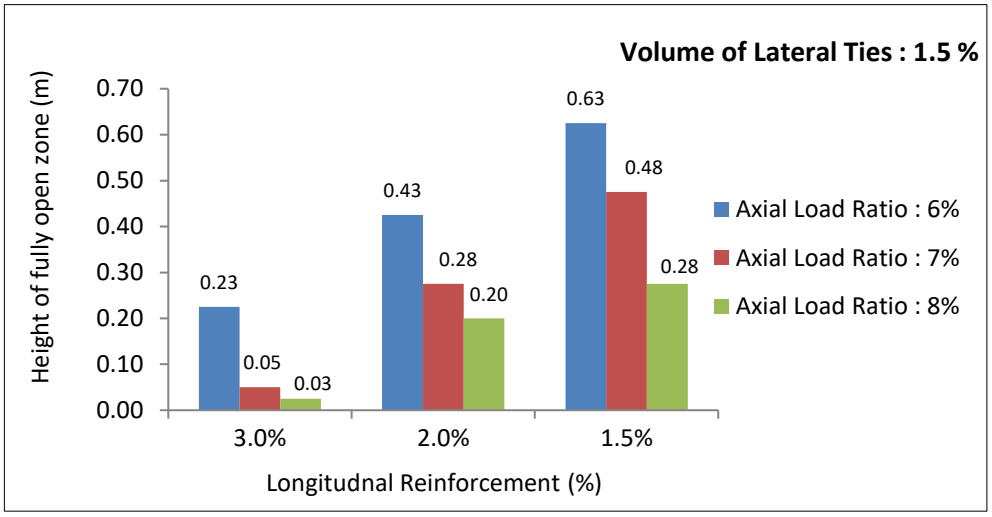


Figure 4.7 Graphical Representation of Results for 1.5% of Lateral Reinforcement.

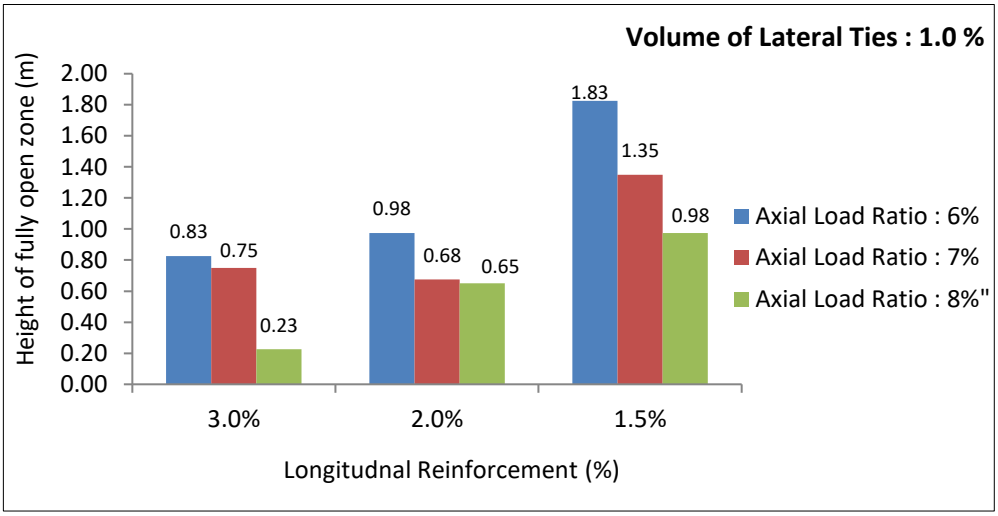


Figure 4.8 Graphical Representation of Results for 1.0% of Lateral Reinforcement.

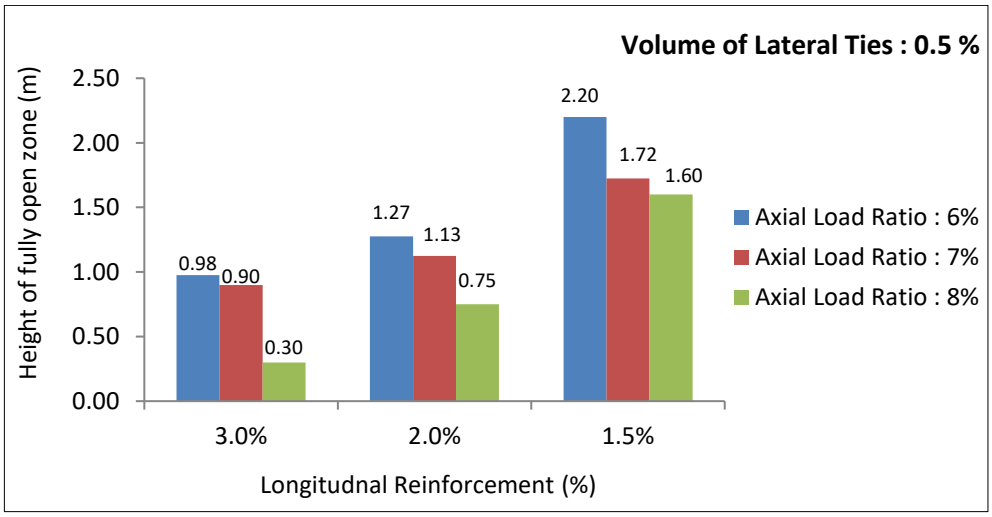


Figure 4.9 Graphical Representation of Results for 0.5% of Lateral Reinforcement.

Table 4.2 Percentage Decrease in Height of Fully Open Zone due to Increase in Lateral Reinforcement.

| Axial Load Ratio | Percentage of longitudinal reinforcement | | |
|---|---|---|---|
| | **3.00 %** | **2.00 %** | **1.50 %** |
| **6.00 %** | 76.5 % | 66.4 % | 71.3 % |
| **7.00 %** | 94.4 % | 75.2 % | 72.2 % |
| **8.00 %** | 90.0 % | 73.3 % | 82.5 % |

## 4.4 RESULTS FOR CONSTANT LONGITUDINAL REINFORCEMENT

In this section the results obtained for all the models are categorized keeping the longitudinal reinforcement constant. From the following graphs it is clearly observed that for a constant percentage of longitudinal reinforcement, the height of fully open zone increases with the decrease in percentage of lateral reinforcement having a particular axial load ratio. Also with the increasing axial load ratio this height of fully open cracked zone further decreases for all percentages of lateral reinforcement considered in this study.

The possible reason for the decrease in height of fully open zone with the increase in axial load ratio from 6% to 8% is a reduction in total stress. The face where this zone is considered is actually the tensile face. As the pier is displaced in the lateral direction (Y-Y) , direct stresses that are tensile in nature due to bending are developed on this face of the pier. The axial load which is applied as pressure load is compressive in nature throughout the height of the pier. Thus, with the increase in axial load ratio , this value of this compressive stress also increases. Hence at particular cross section the total stress which is the net sum of direct tensile stress due to bending and the direct compressive stress due to axial load (opposite in sign to tensile stress) is reduced. Thus, only the portion of concrete where this reduced total stress is more than the stress required to rupture the concrete develops cracks.

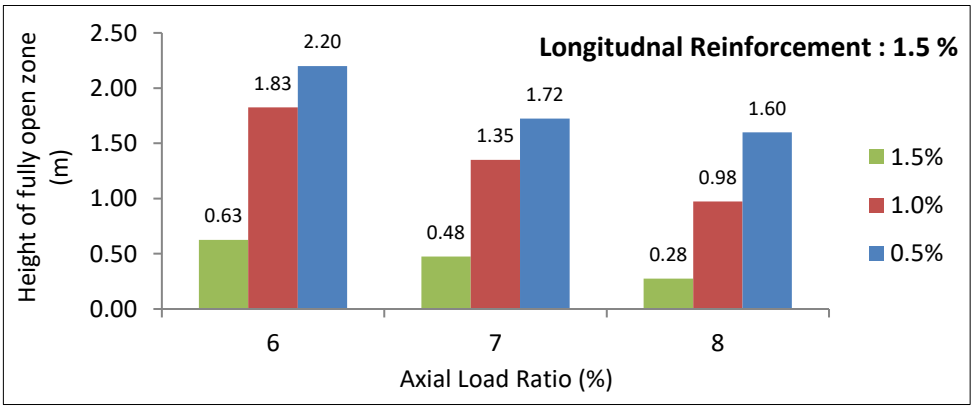


Figure 4.10 Graphical Representation of Results for 1.5% of Longitudinal Reinforcement.

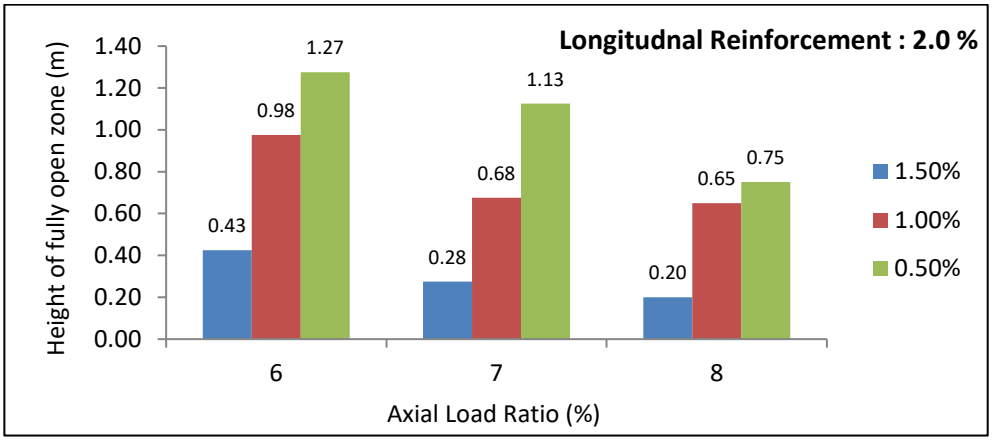


Figure 4.11 Graphical Representation of Results for 2.0 % of Longitudinal Reinforcement.

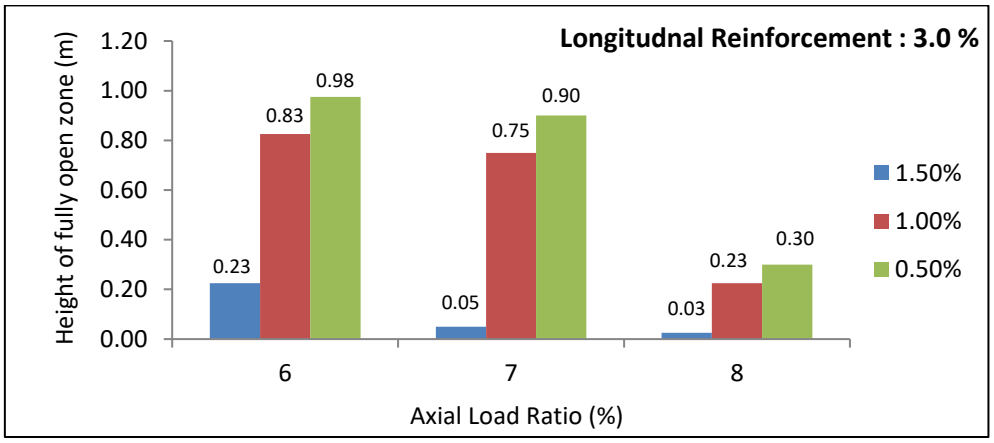


Figure 4.12 Graphical Representation of Results for 3.0 % of Longitudinal Reinforcement.

Table 4.3 shows the percentage decrease in the height of zone of fully open cracked portion with the increase in longitudinal reinforcement from 1.5% to 3%.On an average the decrease in this height is 67 % as the reinforcement is increased in the longitudinal direction.

From the table maximum decrease in the height of cracked zone was observed for the model having minimum lateral reinforcement (i.e. 0.5 %) subjected to higher axial load ratios.

Table 4.3 Percentage Decrease in Height of Fully Open Zone due to Increase in Longitudinal Reinforcement.

| **Percentage of Lateral Reinforcement** | **Axial Load Ratio** | | |
|---|---|---|---|
| | **6.00 %** | **7.00 %** | **8.00 %** |
| **0.5 %** | 65.0 % | 89.6 % | 89.3 % |
| **1.0 %** | 54.6 % | 44.4 % | 76.5 % |
| **1.5 %** | 55.5 % | 47.6 % | 81.2 % |

## 4.4 PLASTIC ZONE HEIGHT

The height of plastic zone for different axial load ratios is shown in following three figures. It was observed that the influence of axial load ratio on plastic zone is very less. With the increase in axial load ratio there was a very less decrease in the height of plastic zone for all the models.

However, as the percentage of longitudinal steel was increased , the height of plastic zone increased by a small amount as can be seen from following figures. It is observed that for a constant longitudinal reinforcement the height of plastic zone either remained constant or decreased with the increase in lateral reinforcement. This decrease in height was very small.

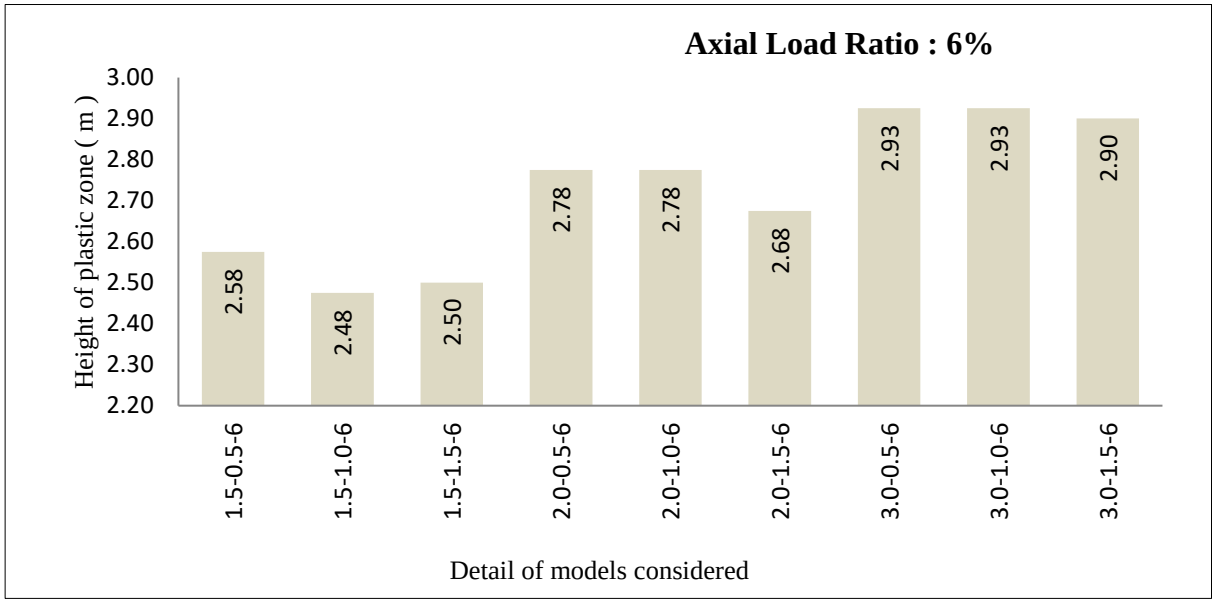


Figure 4.13 Graphical Representation of Plastic Zone Height for Axial Load Ratio 6%

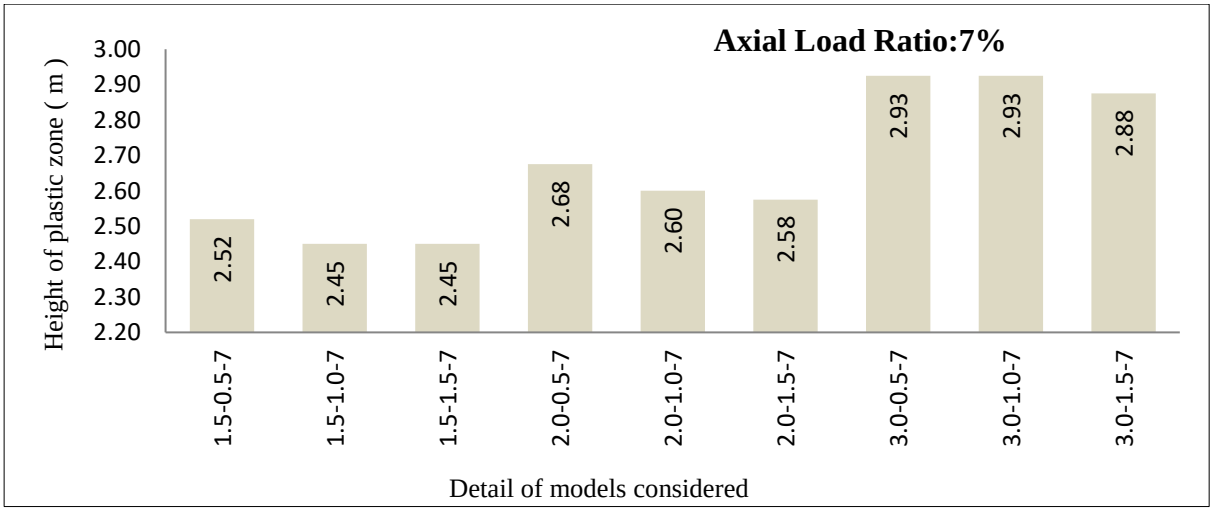


Figure 4.14 Graphical Representation of Plastic Zone Height for Axial Load Ratio 7%

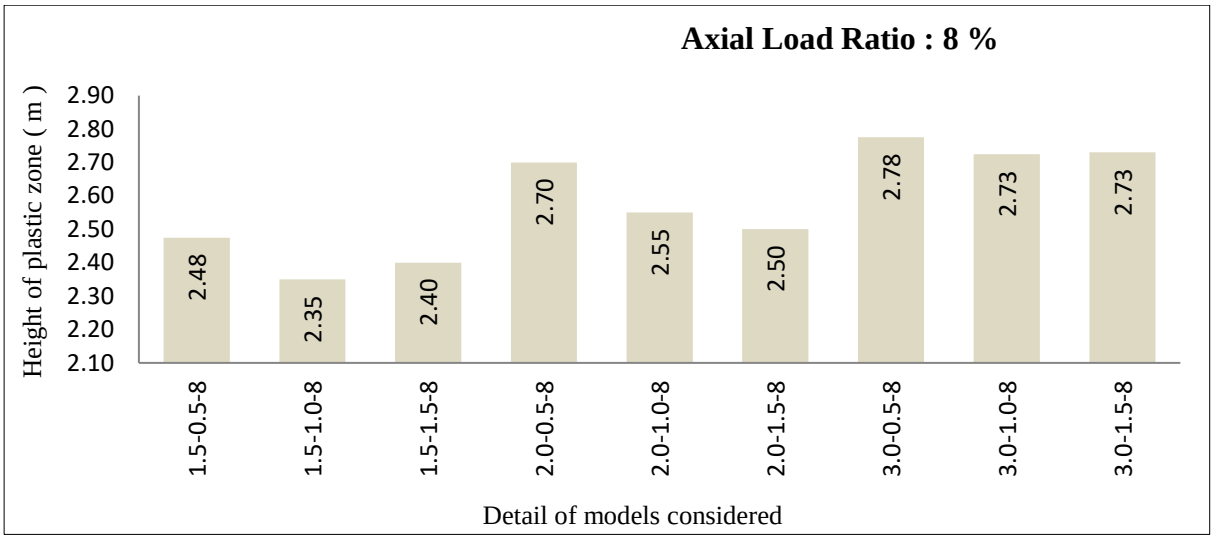


Figure 4.15 Graphical Representation of Plastic Zone Height for Axial Load Ratio 8 %

From the above graphs (Figure 4.13 to 4.15) , it can be concluded that the for a given axial load and a given longitudinal reinforcement , the change in height of plastic zone for models with different lateral reinforcements is very less and a constant plastic zone can be considered on an average.

Plasticity is more or less associated with the stresses more than the elastic limit.These stresses further rely on external loads.In all the twenty seven models the load in the lateral direction was kept constant,only the axial load ratio was varied from 6% to 8% (2.4 to 3.2 N/mm$^2$).Hence the range of total stresses in all the models did not vary considerably,as the variation was only due to the axial loads.Thus not much variation in the plastic zone for different axial load ratios was observed.

The maximum height of the plastic zone from the above three figures was observed as 2.93m and the minimum height of the plastic zone was found to be 2.35m.It can be noted that the difference between the two values is very small ( 0.58 m).

## 4.5 COMPARISON BASED ON CODAL PROVISIONS

From section 1.3 , the maximum height for the zone of lateral confinement as per various international codes is compared with the maximum height of plastic zone obtained in the present study.It is found that for slender pier models analysed in this work , the maximum height of plastic zone (refer Figure 4.13) is more than the values obtained from the codes considered. This leads to the conclusion that these codal provisions are not fully reliable when it comes to slender piers subjected to lateral displacements with axial load acting

simultaneously. Table 4.4 shows the comparison between zone of lateral confinement as per various codes and the maximum plastic zone length obtained after analyzing twenty seven models with varying percentage of lateral and longitudinal reinforcement at different axial load ratios.

Tabel 4.4 Comparison of Max Plastic Zone Length Obtained with Codal Provisions for Zone of Lateral Confinement

| S.No | Code | Max Confinement Length as per code (m) | Max Plastic Zone Length obtained in the present study (m) |
|---|---|---|---|
| 1 | ACI-318-11 | 1.16 | 2.93 |
| 2 | CANADIAN STANDARD (CAN/CSA-A23.3-04) | 1.16 | |
| 3 | AASHTO | 1.75 | |
| 4 | CALTRANS | 1.75 | |
| 5 | NEW ZEALAND STANDARD (NZS 3101) | 1.41 | |
| 6 | EUROCODE 8 (EN1998-2:2005) | 1.41 | |
| 7 | IRC 112:2011 | 1.41 | |

As can be seen from the above table , for a safe design of slender bridge piers a detailed analysis is required, and the possible plastic zone height must be determined analytically and compared with relevant standards. The maximum of the two should be adopted for a safe and stable design.

## 4.6 RESULTS FOR INCREMENTAL LOADING

In the previous section , results for all the twenty-seven models were presented considering direct application of lateral displacement of 25 mm at the top in a single increment. This section includes the output results of nine models on which the top lateral displacement of 25 mm was applied in 5 load steps i.e. with 5 increments along with axial load ratio of 8%.The following table shows the details of lateral displacement applied in each increment at the top in Y-Y direction.

Tabel 4.5 Details of Lateral Displacement Applied at Each Increment

| S No | Increment No | Lateral Displacement Applied in Y-Y direction |
|---|---|---|
| 1 | 1 | 05 mm |
| 2 | 2 | 10 mm |
| 3 | 3 | 15 mm |
| 4 | 4 | 20 mm |
| 5 | 5 | 25 mm |

Three types of results are presented in this section for each increment i.e. height of fully open cracked zone ( red in color) , height of partially open crack zone ( pink in color) and height of plastic zone ( blue in color).The variation in these zones with the variation in longitudinal and lateral reinforcement is discussed in the subsequent sections. Following figure represents the output obtained from MIDAS FEA for each increment of lateral loading and a constant axial load ratio of 8 %.

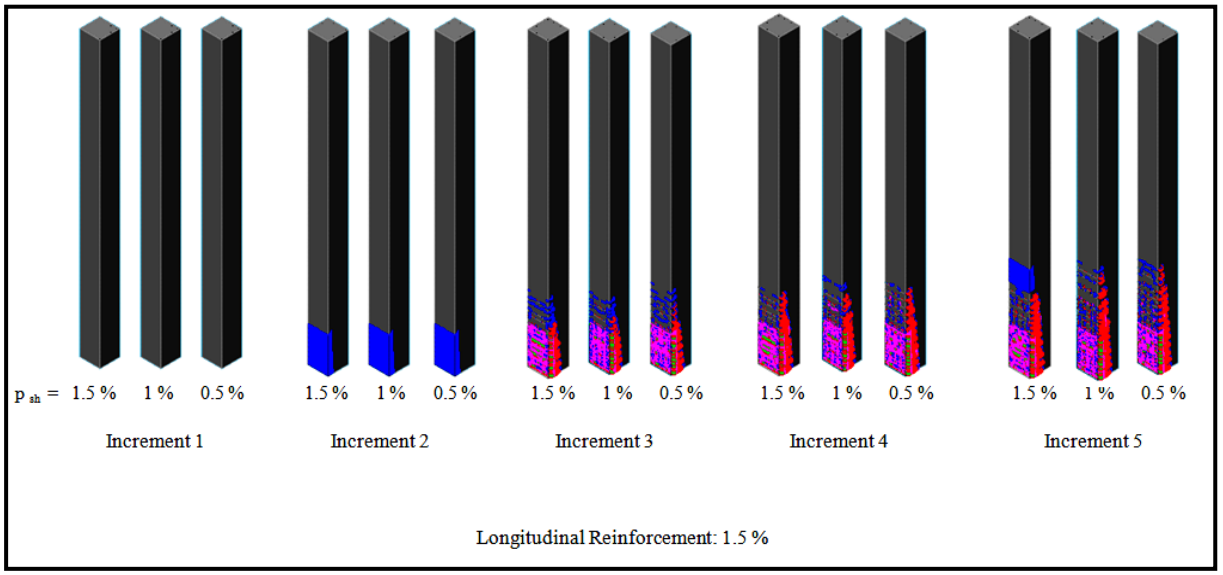


Figure 4.16 Fully Open ( red ) , Partially Open ( pink ) and Plastic Zone ( blue ) for Models Subjected to Incremental Loading with 1.5 % Longitudinal Reinforcement (MIDAS FEA)

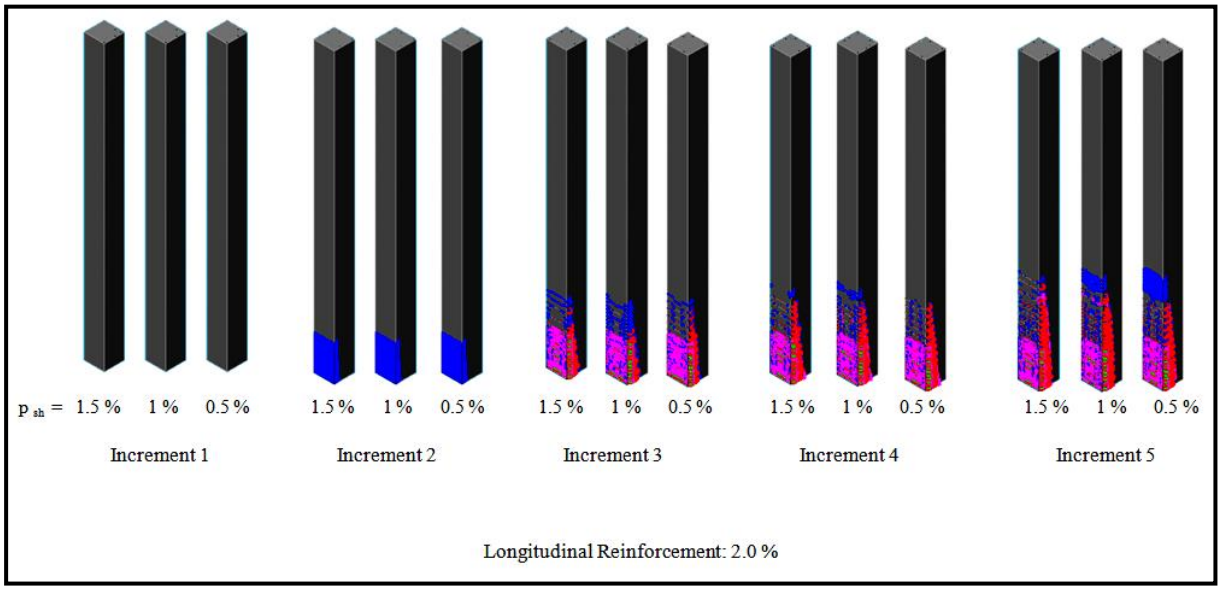


Figure 4.17 Fully Open ( red ) , Partially Open ( pink ) and Plastic Zone ( blue ) for Models Subjected to Incremental Loading with 2.0 % Longitudinal Reinforcement (MIDAS FEA)

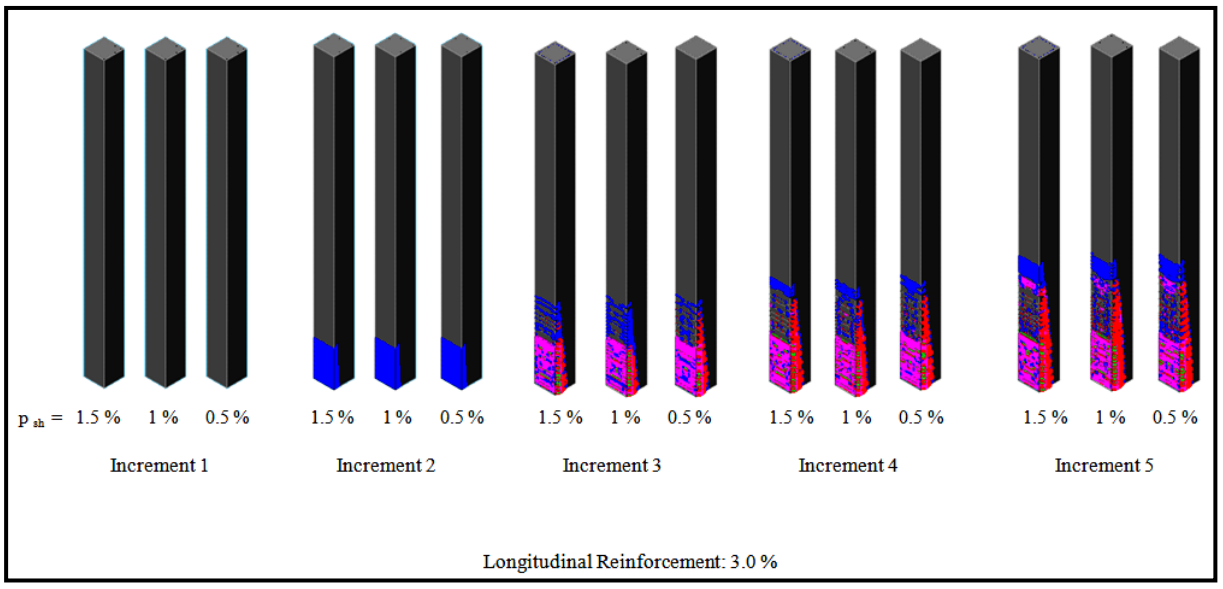


Figure 4.18 Fully Open ( red ) , Partially Open ( pink ) and Plastic Zone ( blue ) for Models Subjected to Incremental Loading with 3.0 % Longitudinal Reinforcement ( MIDAS FEA)

### 4.6.1 Fully Open Cracked Zone

From Figures 4.15 to 4.17 it can be observed that no open cracked zone is formed till increment number 2 for all combinations of lateral and longitudinal reinforcement. However, all three zones are formed for load increment greater than 2.The height of fully open cracked zone increases with the increasing load increments in all the nine models. This is due to the fact that as the incremental step increases the lateral displacement applied at the top of the bridge pier increases , which increases the stresses at the bottom due to increase in moment and hence the height of cracked zone increases. For longitudinal reinforcement ratio of 1.5% , the maximum height of fully open cracked zone is observed in model with minimum shear reinforcement (i.e.

0.50%) at the end of final increment.

In the following curve , it can be observed that the model with lateral reinforcement 1.0 % has lower height of cracked zone than the model having 1.5 % lateral reinforcement at increment number 4 and then increases more than the height of cracked zone for model with 1.50 % lateral reinforcement at the final increment.

For longitudinal reinforcement ratio of 2 % , the height of fully cracked zone is more for model with least lateral reinforcement upto increment step 3 and it is lesser of all at increment level 5 which is contrary to the trend observed in above figure having longitudinal reinforcement as 1.0 %.

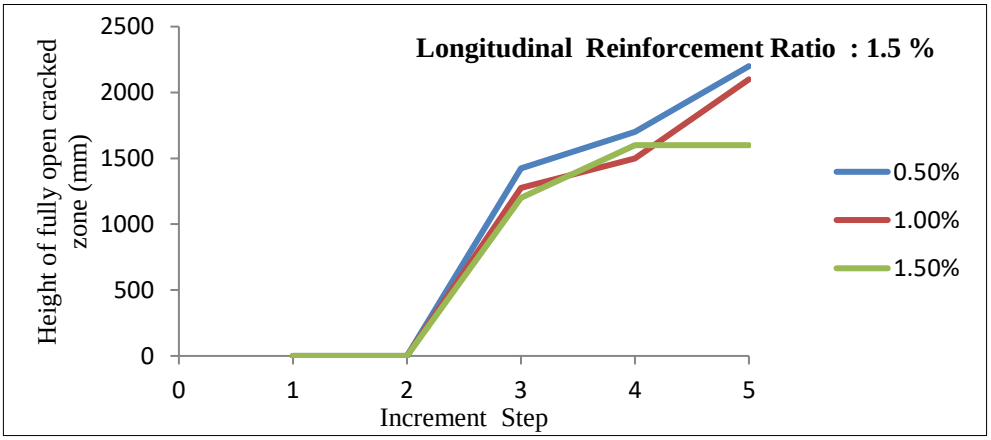


Figure 4.19 Variation of Fully Open Cracked Zone at 1.5% Longitudinal Reinforcement

Also, the model with maximum lateral reinforcement percentage has largest open cracked zone height contrary to Figure 4.18 where it is the lowest for final increment. For load increment 4 almost similar value of height of fully open cracked zone is obtained as can be seen from following figure.

In Figure 4.20, for longitudinal reinforcement ratio of 3 %, almost similar values of fully open cracked zone are obtained at fourth step increment for all percentages of lateral reinforcement. However, for third increment step , the model with least percentage of lateral reinforcement has the highest fully open cracked zone. But for fifth step increment, the model with lateral reinforcement 0.5% has the lowest height of fully cracked zone while other two models have almost similar values for height of fully open cracked zone.

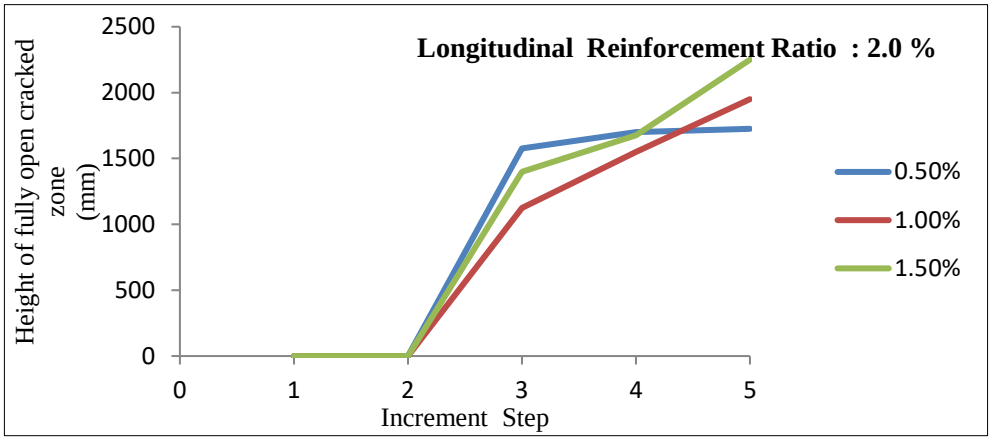


Figure 4.20 Variation of Fully Open Cracked Zone at 2.0% Longitudinal Reinforcement

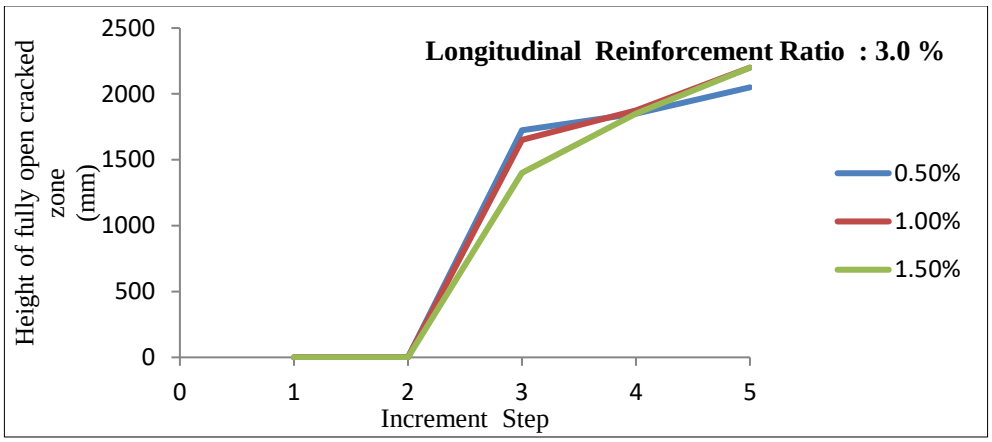


Figure 4.21 Variation of Fully Open Cracked Zone at 3.0 % Longitudinal Reinforcement

From Figures 4.18 to 4.20, only for 1.5 % longitudinal reinforcement, the model with least lateral reinforcement has a higher value for fully open cracked zone length. This is reasonable as the model with 0.50 % lateral reinforcement has a spacing of 152 mm between the ties and hence the space available for the cracked portion of the concrete to fall out is more. If more concrete spalls away the height of fully open zone increases

For other two percentages of longitudinal reinforcement, models with 0.5 % lateral reinforcement have less height of fully cracked zone in comparison to models with lateral reinforcements as 1.0 % and 1.5 %.

### 4.6.2 Partially Open Cracked Zone

Unlike models analyzed for single load increment, some partially open cracks were formed in the models subjected to incremental loading. At constant axial load ratio of 8%, the variation in height of this partially cracked zone for different lateral and longitudinal reinforcement is shown in following graphs.

In all these three graphs no cracking zone was observed till second load step .From Figure 4.21 it can be observed that almost similar heights of partially cracked zone are seen for models with

longitudinal reinforcement of 1.5% corresponding to all percentages of lateral reinforcement. A very slight rise in the height of partially cracked zone is observed with the increasing load step increments. Same trend is seen for models having longitudinal reinforcement as 3%.However for models with longitudinal reinforcement 2 % ,a common height of partially cracked zone for different lateral reinforcement is seen at fourth increment.

For fifth load increment it is observed that the model with lateral reinforcement percentage as 1.5% , the height of partially cracked zone is greater than other models. Also a slight decrease in the partially cracked height is seen for model with 1% lateral reinforcement as the load step changes from fourth to fifth increment.

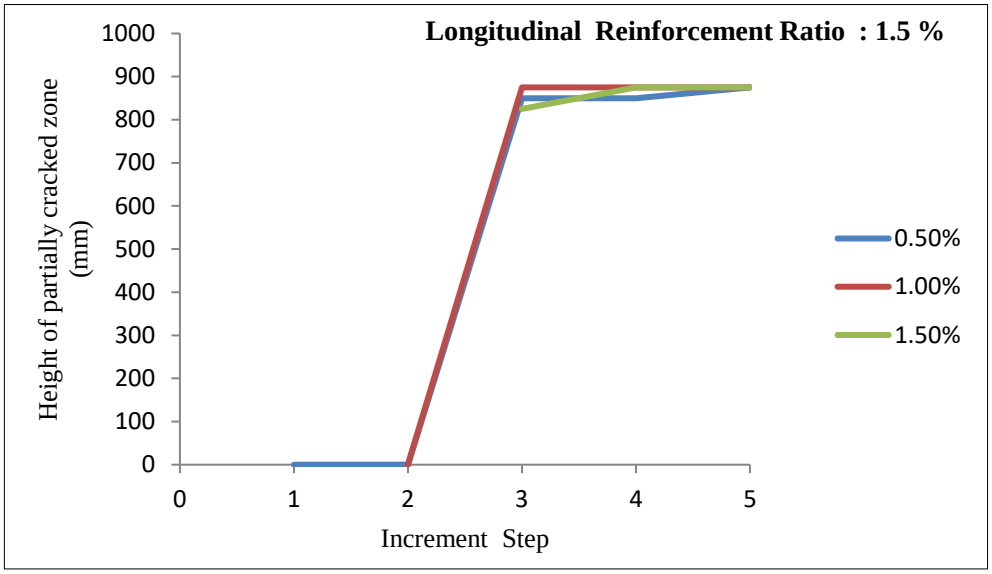


Figure 4.22 Variation of Partially Open Cracked Zone at 1.5% Longitudinal Reinforcement

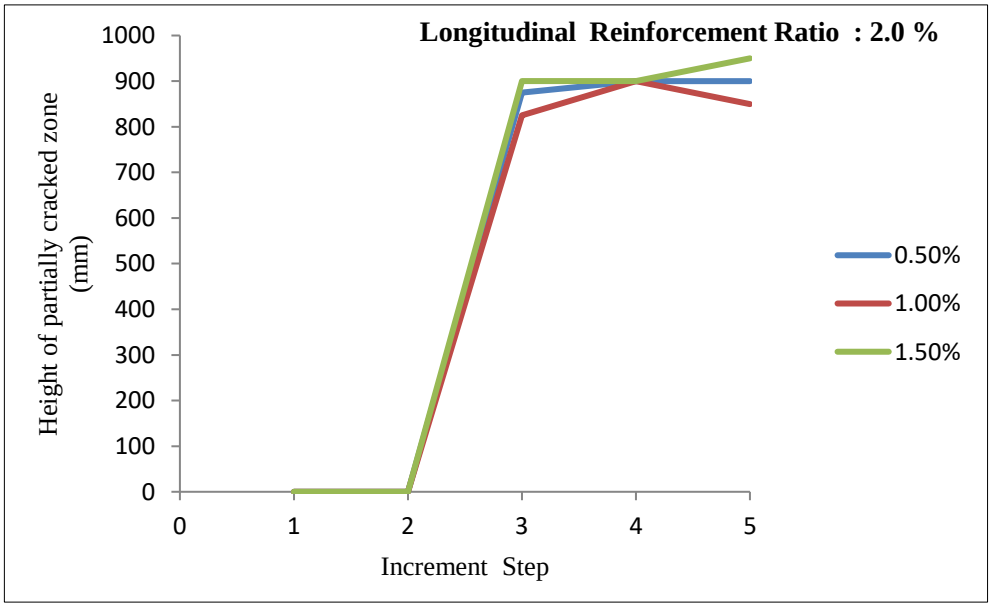


Figure 4.23 Variation of Partially Open Cracked Zone at 2.0% Longitudinal Reinforcement

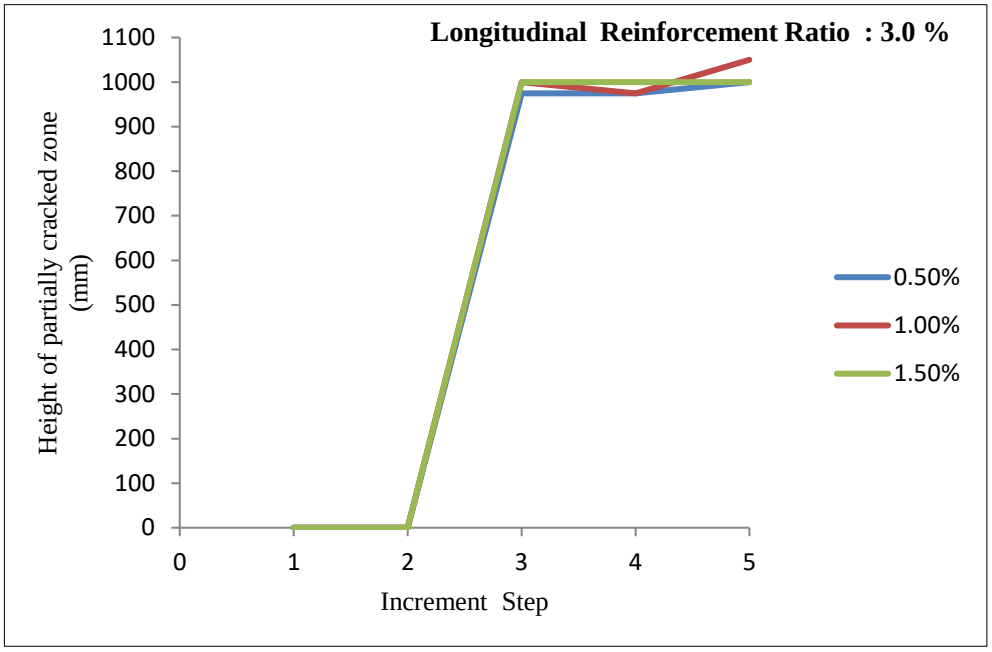


Figure 4.24 Variation of Partially Open Cracked Zone at 3.0% Longitudinal Reinforcement

### 4.6.3 Plastic Zone

Some minimum height of plastic zone for all the nine models considered for incremental loading analysis was observed after first load step increment only ,while the zone of fully cracked portion and partially cracked portion started after second load step increment in all the models.

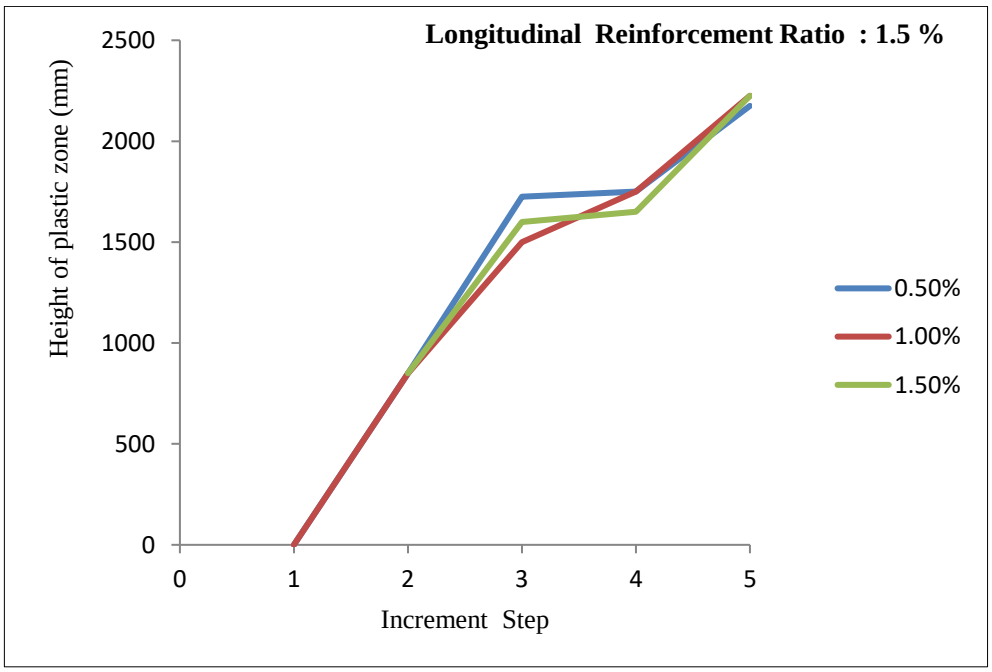


Figure 4.25 Variation of Plastic Zone at 1.5% Longitudinal Reinforcement with Varying Percentages of Lateral Reinforcement

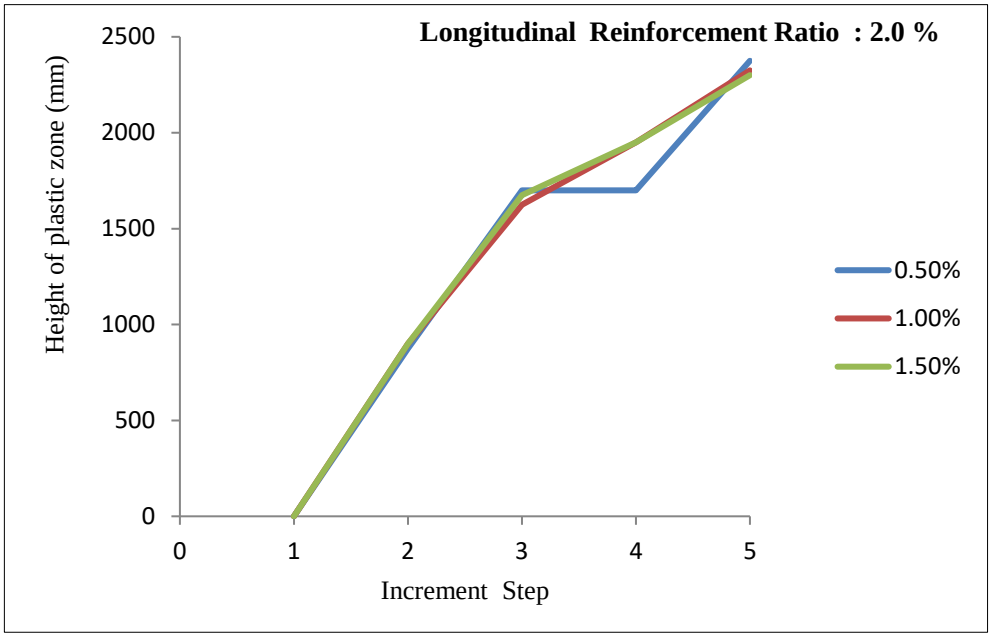


Figure 4.26 Variation of Plastic Zone at 2.0 % Longitudinal Reinforcement with Varying Percentages of Lateral Reinforcement

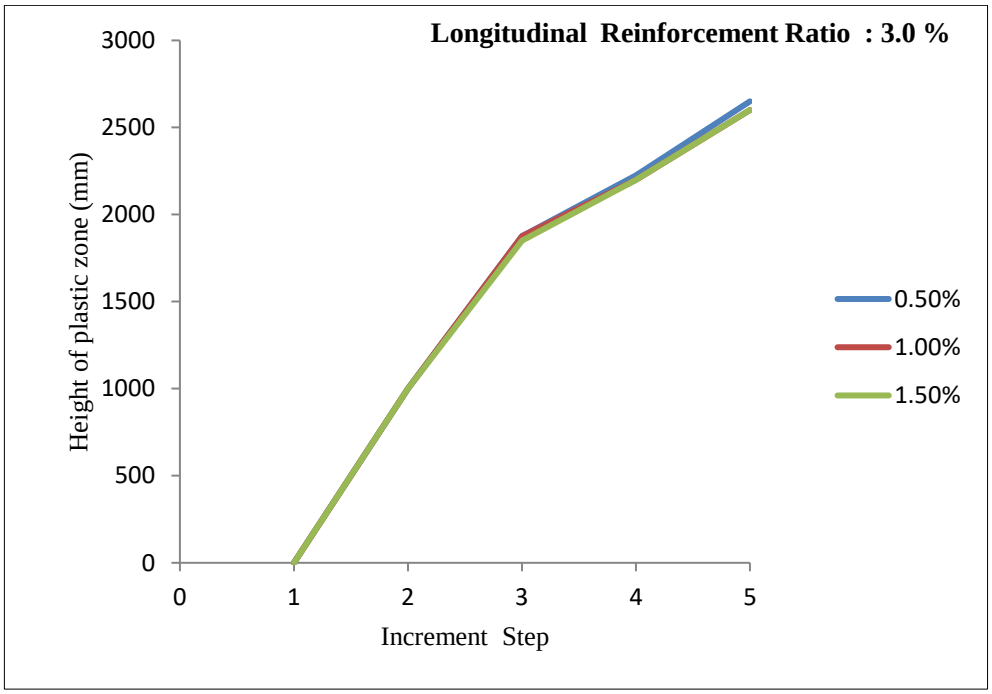


Figure 4.27 Variation of Plastic Zone at 3.0 % Longitudinal Reinforcement with Varying Percentages of Lateral Reinforcement

From Figure 4.24 to 4.26, it can be seen that for models having 1% lateral reinforcement the zone of plastic spread along the pier height continues to increase with the load increments. For 1.5% longitudinal reinforcement, the models with maximum and minimum lateral reinforcement have constant height of plastic zone for increments 3 and 4 and thereafter this height increases for fifth step increment for all percentages of lateral reinforcements considered in this study.

For 2.0% longitudinal reinforcement, it was observed that models with 1.0 % and 1.5 % of lateral reinforcement have a gradual increase in the height of plastic zone as the load increments increase. It was also observed that the plastic zone height remained unchanged for model with least lateral reinforcement at third and fourth load step increment and then it also increased for the fifth increment step.

For all percentages of lateral reinforcement considered in the present study , it was observed that the plastic zone height increases gradually with the increase in the load increment step for models having 3.0% longitudinal reinforcement as shown in figure.

# CHAPTER 5
# CONCLUSION

## 5.1 GENERAL

The nonlinear static analysis performed in the current study has led to certain conclusions for both incremental and non-incremental loading .A general conclusion for all the slender pier models that can be made for both these types of analysis is that the plastic zone above the base of the pier tends to spread beyond the zone of fully cracked portion. A comparison of plastic zone height obtained in this study, with the international guidelines as described in section 1.3 leads to the conclusion that these guidelines need to be revised for the zone of lateral confinement when it comes to slender bridge piers. The conclusions made for both incremental and non-incremental type of analysis has been presented briefly in the following sections

## 5.2 NON-INCREMENTAL LOADING

The conclusions for the twenty-seven models subjected to non-incremental displacement of 25 mm in the Y-Y direction for different axial load ratios and different percentage of lateral and longitudinal steel are presented below :

- With the increase in axial load ratio from 6 % to 8 % keeping other factors constant, the height of fully open cracked zone reduces. As the axial load increases, the direct stress which is compressive in nature also increases on every cross section and it acts in opposite direction to the induced tensile flexural stress at the tensile face of the pier model. Thus, there is a reduction in total stress required for the concrete to rupture. Only that portion of pier develops cracks where this resultant stress is more than the rupture stress required.

- With the increase in percentage of lateral reinforcement in the models, at a particular percentage of longitudinal reinforcement and constant axial load ratio ,the height of fully open cracked zone reduces. However, for a higher percentage of lateral reinforcement the cracked zone along the width of the models ( along X-X direction ) is more. As the percentage of lateral reinforcement is increased, there is a reduction in the spacing between lateral ties provided. With the decrease in spacing, the crushed concrete is effectively confined by these closely spaced ties leaving a lesser area for the cracked concrete to escape out. The concrete may get crushed but could still withstand higher axial loads due to effective confinement provided by lateral ties until it breaks into smaller parts that may escape out through the available area.

- The height of fully open crack zone reduces with the increase in percentage of longitudinal reinforcement for all percentages of lateral reinforcement and for all axial load ratios considered in the study. For a uniform diameter of reinforcing bar (as adopted in the present study),with the increase in percentage of longitudinal reinforcement , the number of bars provided at each face of the pier model increases. Hence this reduces the available area for the cracked concrete to escape out for a particular lateral reinforcement ratio. Thus, the cracked concrete is resisted by more reinforcing bars to spall away avoiding fully open cracks. Also, as the longitudinal reinforcement is increased, the stress induced which remains same for a particular loading gets distributed more effectively at a particular cross section, reducing the stress in the surrounding concrete.

- The height of plastic zone length is very less influenced by the change in axial load ratio. With the increase in lateral reinforcement no increase in height of plastic zone is seen. Instead this height either decreases or remains constant for a constant value of longitudinal reinforcement with increasing lateral reinforcement. For all axial load ratios , the height of plastic zone increases slightly with increasing percentage of longitudinal reinforcement.

### 5.3 INCREMENTAL LOADING

The conclusions for the nine models subjected to incremental displacement of 5 mm in each of the five increments in the Y-Y direction for a constant axial load ratio of 8% and different percentage of lateral and longitudinal steel are presented below :

- For all models, the height of plastic zone increases with the increase in load step increments and after fifth increment the height almost remains same. The zone of plasticity depends predominantly on external loading applied. At the end of increment five, the external loading applied on each model remains same , indicating very less variation of plastic zone for models with different reinforcement percentages.

- For all percentages of longitudinal reinforcement , the height of fully open cracked zone is more for models with least percentage of lateral reinforcement till third load step (i.e 15 mm displacement applied at the top in Y-Y direction).However as the load steps increase from third to fifth, models with minimum lateral reinforcement has a lesser height for longitudinal reinforcement 2 % and 3%

- Only for models having 1.5 % longitudinal steel the height of fully open cracked zone

at almost all load increments, decreases with the increase in percentage of lateral reinforcement. With the increase in percentage of lateral reinforcement, the spacing between ties is reduced leaving lesser space for the cracked concrete to escape out.

- The height of partially open cracked zone increases after second load step increment. For all the nine models this increase is seen only till third step increment after which a nearly constant height is seen for fourth and fifth load increment.

## 5.4 FUTURE SCOPE

In this dissertation , only analytical study was performed on a total of 27 pier models. The experimental validation of the results obtained for various zones considered in this study (like the fully open cracked zone and the height of plastic spread from the base of the pier ) must be done in future to compliment the present work. Also, a detailed analysis in which a diagnostic approach is adopted for evaluation of critical plastic hinge length developed near the pier base could be done. In the present study , only three factors were varied keeping grade of materials constant at a uniform slenderness ratio. The effect of grade of steel and grade of concrete on the height of plastic and crack spread could be done in the future by taking different grades of steel and concrete for a set of pier models. Also, the slenderness ratio of the models could be varied and its corresponding effect on the crack pattern and plasticity status could be assessed in the future.

# REFERENCES


Akiyama M, Suzuki M, Frangopol DM. Stress-Averaged Strain Model for Confined High-Strength Concrete. ACI Structural Journal. 2010 Mar 1;107(2). pp. 179-188.

Babazadeh A, Burgueño R, Silva PF. Evaluation of the critical plastic region length in slender reinforced concrete bridge columns. Engineering Structures. 2016 Oct 15;125:280-93.

Cassese P, Ricci P, Verderame GM. Experimental study on the seismic performance of existing reinforced concrete bridge piers with hollow rectangular section. Engineering Structures. 2017 Aug 1;144:88-106.

Chung JA, Yang IS, Choi SM. Effects of Axial Force on Deformation Capacity of Steel Encased Reinforced Concrete Beam-Columns. Journal of Korean Society of Steel Construction. 2003;15(3):251-9.

Dowell RK, Hines EM. Plastic hinge length of reinforced concrete bridge columns. In Third National Seismic Conference and Workshop on Bridges and Highways: Advances in Engineering and Technology for the Seismic Safety of Bridges in the New Millennium Federal Highway Administration; Oregon, Washington State, California Departments of Transportation; Mid America Earthquake Center; Multidisciplinary Center for Earthquake Engineering Research; Pacific Earthquake Engineering Research Center; and TRB 2002 March 11.

Hines EM, Restrepo JI, Seible F. Force-displacement characterization of well-confined bridge piers. ACI Structural Journal. 2004 Jul 1;101(4):537-48.

Howser R, Laskar A, Mo YL. Effect of Flexural Ductility on Shear Capacity. InStructures Congress 2008: Crossing Borders 2008 (pp. 1-9).

Kim TH, Lee KM, Yoon C, Shin HM. Inelastic behavior and ductility capacity of reinforced concrete bridge piers under earthquake. I: Theory and formulation. Journal of Structural Engineering. 2003 Sep;129(9):1199-207.

Kusuma B, Suprobo P. Investigation of stress-strain models for confinement of concrete by welded wire fabric. Procedia Engineering. 2011 Jan 1;14:2031-8.

Li XL, Sun ZG, Wang DS. Seismic Design for Bridges with Short Piers in High Earthquake Intensity Zones. Journal of Highway and Transportation Research and Development (English Edition). 2013 May 15;7(2):50-5.

Maekawa K, An X. Shear failure and ductility of RC columns after yielding of main reinforcement. Engineering Fracture Mechanics. 2000 Jan 1;65(2-3):335-68.

Li LI, Matsui C. Effects of axial force on deformation capacity of steel encased reinforced concrete beam–columns. InProceedings of 12th world conference on earthquake engineering 2000.

Papanikolaou VK, Kappos AJ. Numerical study of confinement effectiveness in solid and hollow reinforced concrete bridge piers: Analysis results and discussion. Computers & Structures. 2009 Nov 1;87(21-22):1440-50.

Priestley MJ, Park R, Davey BE, Munro IR. Ductility of Reinforced Concrete Bridge Piers. InProc. 6th World Conf. on Earthquake Engineering, New Delhi 1977 Jan.

Reza SM, Alam MS, Tesfamariam S. Lateral load resistance of bridge piers under flexure and shear using factorial analysis. Engineering Structures. 2014 Feb 1;59:821-35.

Ro Y, Yasuo T, Sato N, Yashiro H. Study on the formation of plastic hinges and the failure

of reinforced concrete. Earthquake Engineer 10th World. 1992;5:2977.

Tandon M. Economical design of earthquake-resistant bridges. ISET Journal of earthquake technology. 2005 Mar;42(1):13-20.

Xu S, Wu C, Liu Z, Han K, Su Y, Zhao J, Li J. Experimental investigation of seismic behavior of ultra-high performance steel fiber reinforced concrete columns. Engineering Structures. 2017 Dec 1;152:129-48.

Zahn FA, Park R, Priestley MJ, Chapman HE. Development of design procedures for the flexural strength and ductility of reinforced concrete bridge columns. Bulletin of New Zealand National Society for Earthquake Engineering. 1986 Sep;19(3):200-12.

**BOOKS AND MANUALS :**

Collins, Michael P, and Denis Mitchell (1991) Prestressed concrete structures. Prentice Hall.

Park R,Paulay T Reinforced Concrete Structure (1975) .

MIDAS FEA manual.

**CODES:**

AASHTO, L. R. F. D. "Bridge design specifications." (1998): 5-138.

ACI 318-11 (2012) Building Code Requirements for Structural Concrete and Commentary." American Concrete Institute ; Retrieved 8.

CAN3-A23. 3-M94 (1994) Canadian Standard Association. "Design of concrete structure."

EN 1998-2: (2005) Eurocode, C. E. N. 8: Design of structures for earthquake resistance–Part 2:bridges

IRC 112 (2011) Code of practice for concrete road bridges. Indian Roads Congress

NZS3101:2007, Standards New Zealand, Wellington, NZ.